PLOS PATHOGENS

RESEARCH ARTICLE

Origin and evolution of the zinc finger antiviral protein

Daniel Gonçalves-Carneiro[1], **Matthew A. Takata**[1], **Heley Ong**[1], **Amanda Shilton**[1], **Paul D. Bieniasz**[1,2]*

1 Laboratory of Retrovirology, The Rockefeller University, New York City, New York, United States of America, **2** Howard Hughes Medical Institute, The Rockefeller University, New York City, New York, United States of America

* pbieniasz@rockefeller.edu

Citation: Gonçalves-Carneiro D, Takata MA, Ong H, Shilton A, Bieniasz PD (2021) Origin and evolution of the zinc finger antiviral protein. PLoS Pathog 17(4): e1009545. https://doi.org/10.1371/journal.ppat.1009545

Editor: Welkin E. Johnson, Boston College, UNITED STATES

Received: November 13, 2020

Accepted: April 8, 2021

Published: April 26, 2021

Data Availability Statement: All relevant data are within the manuscript and its Supporting Information files.

Funding: This work was supported by grants from the National Institute of Allergy and Infectious Disease U54AI150470 and R01AI050111 (to PDB) The funders had no role in study design, data collection and analysis, decision to publish, or preparation of the manuscript.

Competing interests: The authors have declared that no competing interests exist.

Abstract

The human zinc finger antiviral protein (ZAP) recognizes RNA by binding to CpG dinucleotides. Mammalian transcriptomes are CpG-poor, and ZAP may have evolved to exploit this feature to specifically target non-self viral RNA. Phylogenetic analyses reveal that *ZAP* and its paralogue *PARP12* share an ancestral gene that arose prior to extensive eukaryote divergence, and the *ZAP* lineage diverged from the *PARP12* lineage in tetrapods. Notably, the CpG content of modern eukaryote genomes varies widely, and *ZAP*-like genes arose subsequent to the emergence of CpG-suppression in vertebrates. Human PARP12 exhibited no antiviral activity against wild type and CpG-enriched HIV-1, but ZAP proteins from several tetrapods had antiviral activity when expressed in human cells. In some cases, ZAP antiviral activity required a TRIM25 protein from the same or related species, suggesting functional co-evolution of these genes. Indeed, a hypervariable sequence in the N-terminal domain of ZAP contributed to species-specific TRIM25 dependence in antiviral activity assays. Crosslinking immunoprecipitation coupled with RNA sequencing revealed that ZAP proteins from human, mouse, bat and alligator exhibit a high degree of CpG-specificity, while some avian ZAP proteins appear more promiscuous. Together, these data suggest that the CpG- rich RNA directed antiviral activity of ZAP-related proteins arose in tetrapods, subsequent to the onset of CpG suppression in certain eukaryote lineages, with subsequent species-specific adaptation of cofactor requirements and RNA target specificity.

Author summary

To control viral infections, cells have evolved a variety of mechanisms that detect, modify and sometimes eliminate viral components. One of such mechanism is the Zinc Finger Antiviral Protein (ZAP) which binds RNA sequences that are rich in elements composed of a cytosine followed by a guanine. Selection of viral RNA can only be achieved because such elements are sparse in RNAs encoded by human genes. Here, we traced the molecular evolution of ZAP. We found that *ZAP* and a closely related gene, *PARP12*, originated from the same ancestral gene that existed in a predecessor of vertebrates and invertebrates. We found that ZAP proteins from mammals, birds and reptiles have antiviral activity but

only in the presence of a co-factor, TRIM25, from the same species. ZAP proteins from birds were particularly interesting since they demonstrated a broader antiviral activity, primarily driven by relaxed requirement for cytosine-guanine. Our findings suggest that viruses that infect birds–which are important vectors for human diseases–are under differential selective pressures and this property may influence the outcome of interspecies transmission.

Introduction

Organisms have evolved numerous mechanisms to detect and control viral infections. For example, pattern recognition receptors (PRRs), including RIG-I-like receptors and Toll-like receptors, can recognize RNA or DNA structures that are uniquely present or inappropriately localized in virus-infected cells [1]. Recognition by PRRs triggers a signalling cascade that culminates in the increased transcription of many so-called interferon-stimulated genes (ISGs), some of which encode effectors with direct antiviral properties [2]. PRRs, signalling molecules and direct antiviral effectors often exhibit species-dependent sequence and functional divergence, as a consequence of extreme reciprocal selective pressures placed on hosts and the viruses that colonize them [3].

The zinc finger antiviral protein (ZAP) is unusual in that it combines features of a nucleic acid PRR and a direct antiviral effector. ZAP was initially found to inhibit the replication of broad range of unrelated viruses, and to act by destabilizing viral RNA [4–6]. Human ZAP is composed of three structural domains: an N-terminal RNA-binding domain that has four CCCH-type zinc fingers, a central domain that has an additional CCCH-type zinc finger plus two WWE domains, and a C-terminal poly(ADP-ribose)-polymerase (PARP)-like domain. ZAP requires certain cofactors for its antiviral activity, including TRIM25, a E3 ubiquitin ligase that interacts with ZAP via its SPRY domain [7,8]. However, the precise role of TRIM25 in ZAP function is unknown. Several helicases and ribonucleases, including the putative endonuclease KHNYN, have also been reported to be required for ZAP activity [9,10].

We recently showed that ZAP targets particular RNA elements based on their dinucleotide composition [11]. Specifically, ZAP binds directly to RNA elements that contain CpG dinucleotides, and RNAs that contain CpG-rich sequences exhibit cytoplasmic depletion in the presence of ZAP. X-ray crystal structures of the N-terminal RNA binding domain in a complex with an RNA target have revealed that the specificity of ZAP for CpG dinucleotides is conferred by a binding pocket positioned within a larger RNA binding domain [12,13]. This pocket can only accommodate CpG dinucleotides, and its integrity is required for specific binding to CpG-rich RNA. Accordingly, the CpG content of viral genomes predicts their sensitivity/resistance to ZAP [11].

Human ZAP has minimal effects on the host transcriptome, presumably because CpG dinucleotides have been largely purged from the human genome, rendering human mRNAs largely ZAP-resistant. The purging of CpG dinucleotides (or 'CpG-suppression') from host genomes has occurred through DNA methylation followed by spontaneous deamination at CpG dinucleotides over millions of years and to varying degrees in different lineages [14]. A commonly accepted theory that would enable this phenomenon argues that the emergence of DNA methyltransferases–enzymes that catalyse the conversion of cytosines in a 5'-cytosine-guanine-3' (CpG) context to 5-methyl-cytosine–led to increased levels of methylated CpG. While spontaneous deamination of the methylated cytosine generates thymine, an authentic DNA base, deamination of an unmethylated cytosine generates deoxyuridine, that would be

repaired. Thus, many DNA genomes have become purged of CpG dinucleotides and enriched in TpG dinucleotides [15].

Remarkably, the genomes of many RNA viruses are CpG-poor, and to a large extent CpG suppression in host is mirrored by CpG suppression in the viruses that colonize them. This feature is true even for RNA viruses whose genome composition could not have been shaped by DNA methylation/deamination. The selective pressures that led to CpG suppression in viral genomes remain unknown, but long-term adaptation to hosts in which a selective pressure was imposed by ZAP is a likely possibility.

Here we investigated the origins of ZAP and its CpG-specific antiviral activity. A paralogue of *ZAP*, *PARP12*, exists that also lacks poly(ADP-ribose) polymerase activity, but catalyses the addition of mono(ADP-ribose) to proteins [16]. Like ZAP, PARP12 also contains five CCCH-type zinc fingers, two WWE domains and has been reported to exhibit antiviral activity against several RNA viruses including vesicular stomatitis virus (VSV), encephalomyocarditis virus (ECMV) and Dengue virus [17–19]. Since *ZAP* and *PARP12* share domain and sequence homology, it is likely that these antiviral genes have shared the same ancestral gene. However, when this gene duplication occurred and when specific CpG-binding affinity of ZAP-like proteins emerged remains unknown. We examined the genomes of vertebrates and invertebrates for gene products with sequence and domain homology to ZAP/PARP12. Phylogenetic analysis of *ZAP/PARP12*-related sequences showed that these genes arose early in the divergence of vertebrates and have their origin in an ancestral gene whose descendants are present in some modern invertebrates, such as cnidarians, but absent in others, such as arthropods. Each of the ZAP-related proteins from tetrapods that were examined showed antiviral activity against CpG-enriched HIV-1 when overexpressed in human cells. Notably, in some cases co-expression of a cognate TRIM25 protein in human cells was essential for the activity of ZAP proteins from non-mammalian species (e.g., chicken and alligator) suggesting that these proteins have co-evolved. Finally, we found that while CpG targeting specificity is common among ZAP proteins of human, mouse, bats and alligator origin, ZAP proteins of avian origin were less specific for CpG enriched targets and inhibited the replication of both wild type and mutant HIV-1. These data suggest lineage-specific evolution of ZAP and its cofactors with distinct non-self RNA targeting abilities that could influence the host range of viruses with zoonotic potential.

Results

The dinucleotide composition of mRNAs and the origin of *ZAP*-like genes

To understand the evolutionary origins of ZAP-mediated, CpG-rich RNA targeted, non-self RNA recognition, we first mined vertebrate and invertebrate genomes for gene products with sequence homology to human ZAP. In the human genome, a *ZAP* homolog, *PARP12*, that shares several features with ZAP including five CCCH-type zinc fingers, two WWE domains and a C-terminal PARP domain (**Figs 1A and S1A and S1B**), is found at a proximal location on chromosome 7 (**Fig 1B**), suggesting that *ZAP* and *PARP12* are paralogs that arose from a common ancestor. A related gene termed 'ZAP-like' is present on human chromosome 7 but contains sequences corresponding only to the ZAP N-terminal RNA binding domain (**Figs 1A and S1A–S1C**). For searches of other genomes we considered sequences that contained five CCCH-type zinc fingers and a WWE domain in a ZAP/PARP12-like configuration (**Fig 1A**). Most of the sequences revealed by blast searches also encoded PARP-like domains, in common with ZAP and PARP12, but the PARP domain was lacking in ZAP/PARP12 sequences from a few species. The topology of a phylogenetic tree constructed using ZAP/PARP12 protein sequences revealed two separate lineages in vertebrates and invertebrates (**Fig 1C**) suggesting that a gene that is ancestral to modern *ZAP/PARP12* originated prior to the divergence of

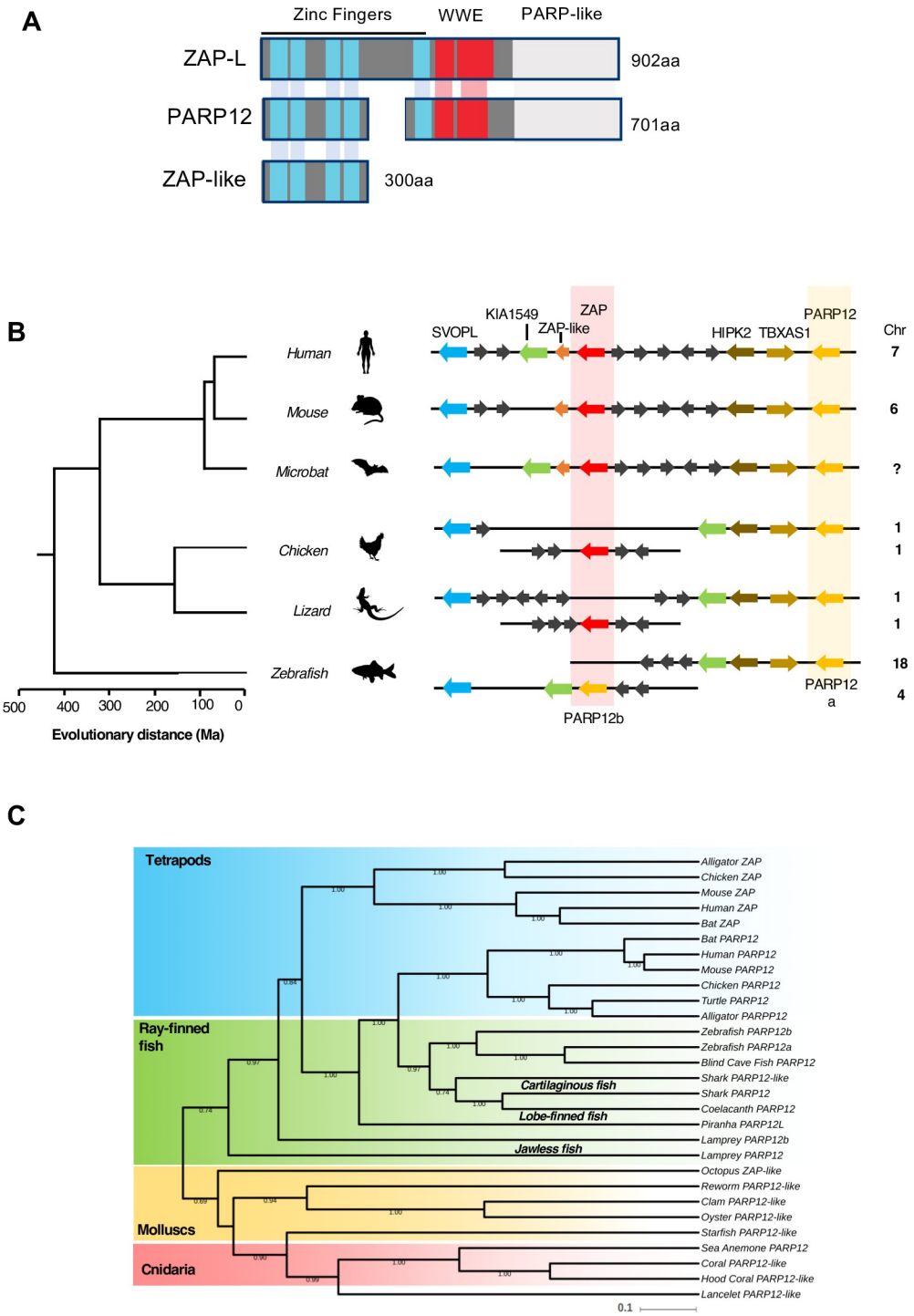

Fig 1. ZAP and PARP12 share a common ancestor. (A) Schematic representation of the domain organization of human ZAP and its paralogues PARP12 and ZAP-like. (B) Diagrams of the organization of PARP12 (in yellow) and ZAP (in red) loci in vertebrate genomes generated using multiple genome browsers (NCBI, Ensembl, Genomicus). Evolutionary distance of the indicated species (presented in million years, Ma) is based on [36]. Chr, chromosome number. (C) Maximum likelihood tree (midpoint rooted) depicting phylogenetic relationships among *PARP12*- and *ZAP*-related genes in vertebrate and invertebrate species, generated with BEAST and 1000 bootstrap replicates. Shaded areas loosely clustered sequences from related species in the superclass Tetrapoda (in blue), clade Actinopterygii (Ray-finned fish, in green), the phylum Mollusca (molluscs, in yellow) and the phylum Cnidaria (in red).

https://doi.org/10.1371/journal.ppat.1009545.g001

cnidarians from other animals, approximately 650 million years ago. While *ZAP/PARP12*-related sequences were found in several invertebrate genomes, the *Arthropoda* phylum, which includes insects and nematodes, appeared to lack *ZAP/PARP12* homologs, suggesting loss of *ZAP/PARP12* in this lineage.

Invertebrate genomes typically contained only one copy of a *ZAP/PARP12*-related gene, while vertebrates had two (Fig 1B and 1C). One set of *ZAP/PARP12* related sequences were more closely related to PARP12, and appeared to be represented once in tetrapod genomes and several fish genomes (**Figs** 1B and 1C **and** S1D). In the case of teleost fish, several *ZAP/PARP12*-related sequences were found, including PARP12a, PARP12b and ZC3HDC1L (S2A Fig). Phylogenetic analysis showed that *ZC3HDC1L* is unique to teleost fish and it is equally distantly related to tetrapod *ZAP* and *PARP12* (S2A Fig). This gene has a unique feature that is not shared by any paralogue of *ZAP* and *PARP12* of all the species that we studied, which is that it contains an additional domain located at the C-terminus of the PARP-like domain (S2B Fig). Since *ZC3HDC1L* is only found in teleost fish, we excluded this gene from our analysis, however it is likely that the whole-genome duplication that occurred in teleost fish preserved at least three *ZAP/PARP12*-related sequences in some fish lineages (S2C Fig). A clearly distinguishable set of *ZAP/PARP12* genes emerged exclusively in tetrapods, and this linage contained the human *ZAP* gene that has been demonstrated to exhibit antiviral activity against CpG-rich viruses (Fig 1C). Within tetrapods, the *ZAP*-related genes were more diverse in sequence than the PARP12-related sequences (**Figs** 1C **and** S1D Fig). Overall these data suggest that ZAP originated in tetrapods from the duplication of an ancestral *PARP12* gene, and that *ZAP* may have been under stronger diversifying selective pressure than *PARP12* [20].

Consistent with the aforementioned scenario, *ZAP* is located at about 900kb upstream of *PARP12* in mammalian genomes, while *ZAP* and *PARP12* are further apart but on the same chromosome in reptilian and avian genomes (Fig 1B). In the zebrafish genome, duplicated *PARP12a* and *PARP12b* genes are located on two different chromosomes (18 and 4, respectively, Fig 1B). The *PARP12a* locus resembles the *PARP12* locus in birds and reptiles while the *PARP12b* locus resembles that of *ZAP* in mammalian genomes (Fig 1B). Thus, even though CpG-suppression is commonly observed among vertebrates, the genes most closely related to human *ZAP* are found only in tetrapods (mammals, birds and reptiles).

Human PARP12 does not recognize or inhibit expression from CpG-rich RNA

Since ZAP and PARP12 share an ancestral origin and are structurally related (Fig 1), we inquired if PARP12 also had antiviral activity against CpG-enriched HIV-1. To assess this, we measured the infectious virus yield and viral protein expression in HEK293T ZAP$^{-/-}$ cells co-transfected with wild-type HIV-1 (HIV-1$_{WT}$) or CpG-enriched mutant (HIV-1$_{CG}$) proviral plasmids and increasing amounts of plasmids encoding either the long isoform of human ZAP (ZAP-L) or human PARP12. Expression of ZAP-L reduced HIV-1$_{CG}$ Env levels and the yield of infectious HIV-1$_{CG}$ but did not affect HIV-1$_{WT}$, as expected, but PARP12 had no effect on the yield or protein expression by either virus (Fig 2A and 2B). To test effects on other CpG-enriched or CpG-suppressed virus derived sequences, we used a luciferase-based reporter system in which ZAP or PARP12 expression plasmids were cotransfected with a plasmid encoding the firefly luciferase gene and a 3' UTR containing vesicular stomatitis virus (VSV) or influenza A virus (IAV) derived sequences (Fig 2C). Plasmids that encoded CpG-enriched derivatives of these sequences were included in the experiment [11]. Overexpression of ZAP specifically reduced the expression of the reporter gene with CpG-enriched 3'UTR sequences; however, PARP12 had no effect (Fig 2C). Thus, while they are structurally related, PARP12

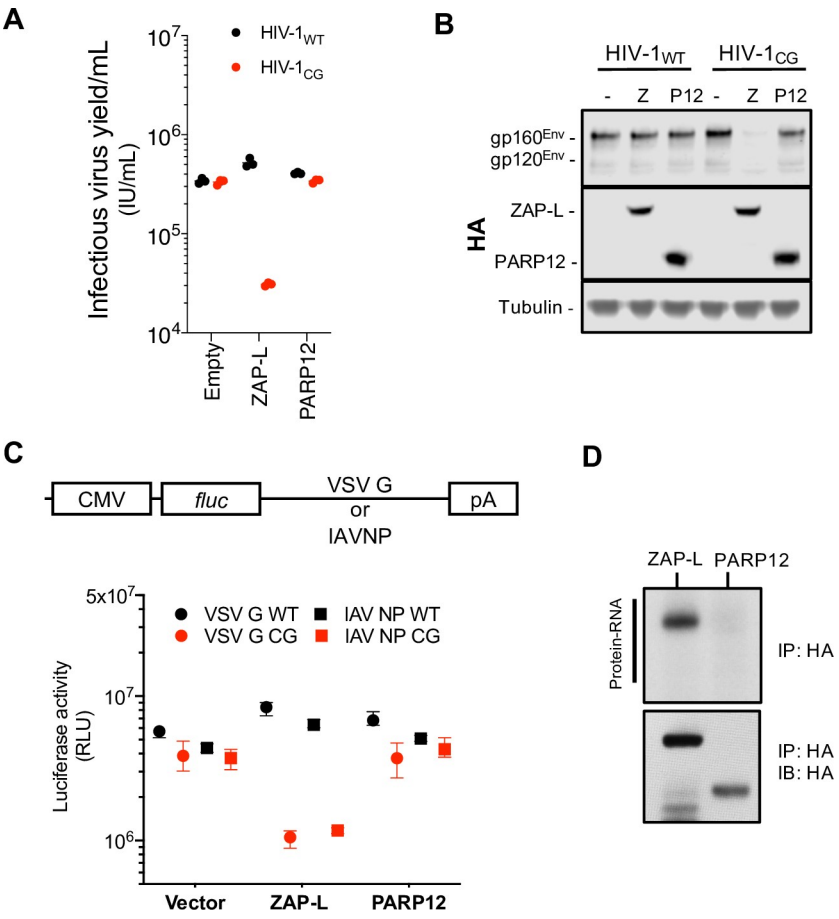

Fig 2. Human PARP12 does not restrict CG-rich viruses. (A-B) HEK293T ZAP$^{-/-}$ cells were transfected with HIV-1_{WT} or HIV-1_{CG} plasmids and plasmids encoding human ZAP-L-HA or PARP12-HA. Supernatant was harvested after 48h and the infectious virus yield was determined using MT4-R5-GFP target cells (A). Whole cell lysates were analysed by western blotting (B). IU, infectious units. (C) HEK293T ZAP$^{-/-}$ cells were transfected with plasmids encoding a luciferase reporter gene that contained VSV-G wildtype (WT) or CG-enriched (VSV-G CG) sequences, or IAV-NP WT or CG-enriched sequences as 3' UTRs, together with plasmids expressing ZAP-L, PARP12 or an empty plasmid (vector). RLU, relative light units. (D) HEK293T ZAP$^{-/-}$ cells were transfected with plasmids expressing ZAP-L-3xHA or PARP12-3xHA and 24h later culture medium was supplemented with 100μM 4SU. After overnight incubation cells were irradiated with UV light, and ZAP-L/PARP12 were immunoprecipitated. RNA bound to each protein was radiolabeled and protein-RNA adducts were resolved by SDS-PAGE, transferred to a nitrocellulose membrane and exposed to autoradiographic film. In parallel, a western blot of immunoprecipitated proteins was done using anti-HA antibody. IP, immunoprecipitation. IB, immunoblot.

https://doi.org/10.1371/journal.ppat.1009545.g002

does not share the same antiviral activity as ZAP. Differences in antiviral activity or specificity may be attributable to variation in RNA-binding activity, as ZAP:RNA adducts were easily detected in crosslinking immunoprecipitation assays, while PARP12:RNA adducts were undetectable under the same experimental conditions (Fig 2D).

These data suggest the that CpG-specific antiviral activity emerged concurrently with or after the emergence of the ZAP-like genes from a ZAP/PARP12 ancestral progenitor. To assess whether the emergence of ZAP-like proteins was potentially enabled by the prior presence CpG suppression in eukaryotic genomes, we generated an *in silico* library of open reading frames (ORFs) and 3'UTRs from organisms across the tree of life, including: vertebrates, nematodes, insects, molluscs and plants. We first calculated the frequency distribution (observed/expected) for each of the 16 possible dinucleotides in ORFs (Fig 3A). Notably, dinucleotide

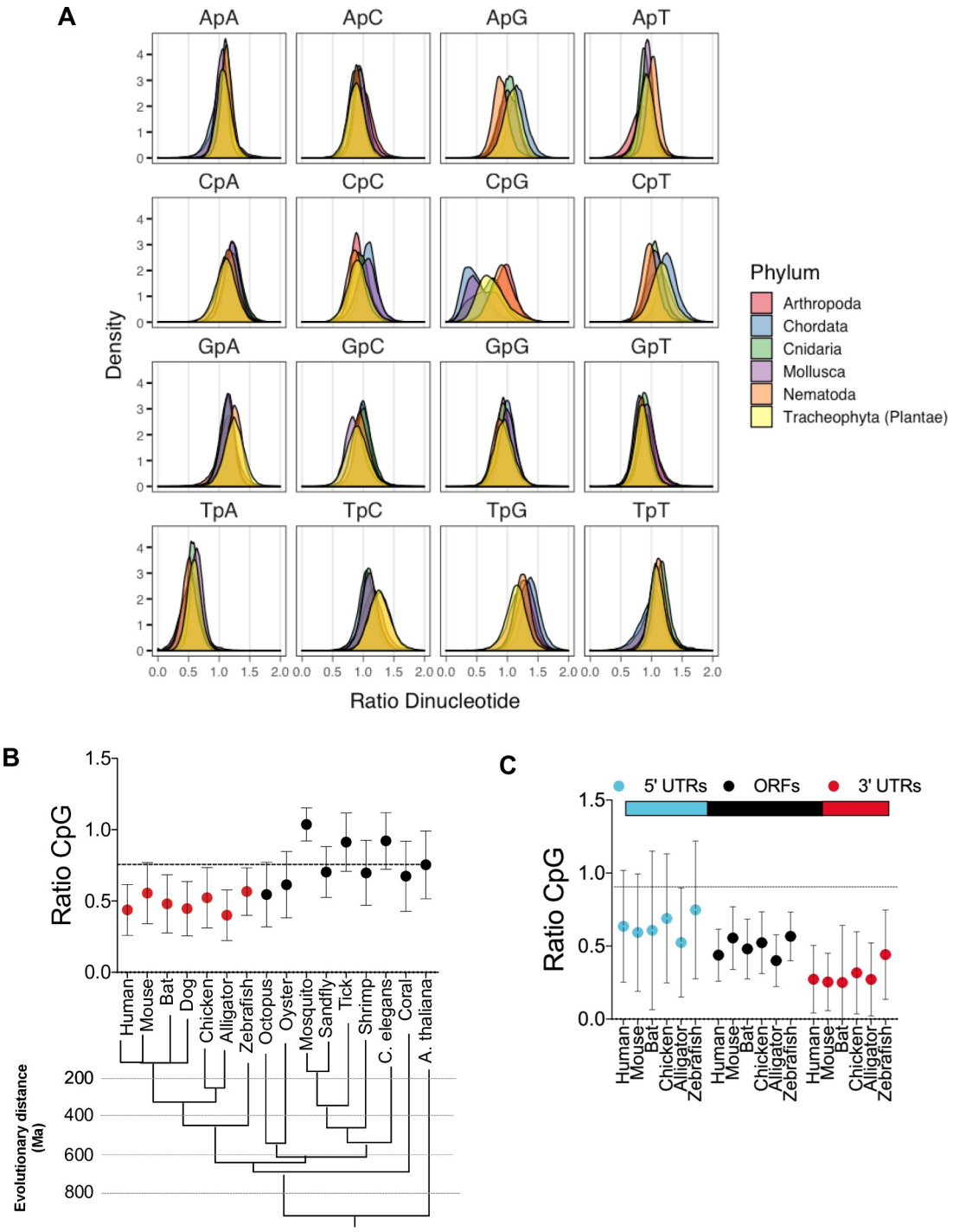

Fig 3. RNA transcripts from vertebrates are CpG-suppressed. (A) Open reading frames (ORFs) from several organisms belonging to the indicated phyla were collected from the NCBI nucleotide database and dinucleotide frequency ratio (observed/expected) was calculated and frequency distribution for each dinucleotide in ORFs was plotted. (B) Average dinucleotide observed/expected ratio in various animal species. Evolutionary distance (presented in million years, Ma) of indicated species was based on [36]. (C) Average dinucleotide observed/expected ratio in various portions of vertebrate mRNA transcripts vertebrates.

https://doi.org/10.1371/journal.ppat.1009545.g003

frequencies among distantly related species were similar, with the exception of the dinucleotide CpG. Specifically, ORF sequences from arthropods and nematodes had CpG frequencies close to that expected based on their mononucleotide compositions. Conversely, CpG dinucleotides were suppressed in vertebrates (*Chordata*) and molluscs (*Mollusca*) (**Fig 3A and 3B**). CpG suppression was even more evident in vertebrate mRNA 3'UTRs (**Figs 3C and S3A**), while the presence of CpGs in 5'UTRs was variable, more so than any other dinucleotide, perhaps reflecting the comparatively short length of many 5'UTRs and a role for RNA structure in translation regulation (**Fig 3C**). Overall, these data indicate that CpG-suppression is observed primarily in vertebrates, is not specific to coding sequences, and was likely present in animals prior to the emergence of genes closely related to the human ZAP CpG-specific antiviral gene.

ZAP proteins from tetrapods have antiviral activity, but some require a cognate TRIM25

We next assessed whether the ZAP-related genes from tetrapods that share the highest homology with human ZAP exhibit CpG-targeted antiviral activity. During initial experiments, we found that the full-length ZAP proteins from various species were expressed at inconsistent levels in human cells (**S4A Fig**). Therefore, in an attempt to circumvent this confounding variable, we constructed plasmids expressing chimeric proteins in which the N-terminal zinc finger domains of mouse, bat, chicken and alligator ZAPs were fused to the remaining portions (including the WWE and PARP-like domains) of human ZAP (**Fig 4A**). Importantly, the isolated N-terminal domain of ZAP has been reported to be sufficient for antiviral activity [4] and is responsible for RNA recognition. By constructing these chimeras we aimed to maintain the RNA-binding specificity of ZAP proteins while also maintaining the putative regulatory functions of the WWE and PARP-like domains of human ZAP. All ZAP chimeras had equivalent expression and localization as demonstrated by western blot analysis and immunofluorescent microscopy (**S4A and S4B Fig**). To test the activity of these chimeric proteins, we first transfected HEK293T ZAP$^{-/-}$ cells with proviral plasmids and increasing amounts of plasmids encoding the various ZAP chimeras. Chimeric ZAP proteins with N-terminal domains (NTDs) from human (huZAP) and bat (baZAP) had antiviral activity against HIV-1_{CG}, while ZAP chimeras with NTD's derived from alligator (alZAP) and mouse (moZAP) were less potent, the ZAP chimera with an NTD from chicken (chZAP) had little or no antiviral activity (**Fig 4B and 4C**).

The failure of the non-mammalian ZAP NTD chimeras to function in human cells could have been due to an absence of RNA recognition activity, or incompatibility with a required cofactor in human cells. One important co-factor for ZAP is TRIM25 [7,8]. Even though HEK293T ZAP$^{-/-}$ cells express TRIM25, the nature of the TRIM25-ZAP interaction and specifically, the ZAP domain with which TRIM25 functionally interacts is unknown.

Therefore, we explored whether the ZAP NTD interacts with TRIM25. Experiments in which ZAP-L and TRIM25 were overexpressed in HEK293T ZAP$^{-/-}$ TRIM25$^{-/-}$ cells (**Figs 5A and S5A**) revealed that ZAP and TRIM25, could be co-immunoprecipitated, as previously reported [7]. Removing the TRIM25 SPRY domain (one truncated form was composed of the N-terminal 371 amino acids and the other was composed of the N-terminal 410 amino acids) dramatically reduced the HIV-1_{CG} -specific antiviral activity of ZAP (**Fig 5B**), as well as the ability of TRIM25 to co-immunoprecipitate with ZAP, again consistent with prior reports (**Fig 5A and 5B**) [7]. Next we conducted coimmunoprecipitation experiments in which the ability of full-length human ZAP-L, a truncated form of ZAP lacking the NTD (ΔZnF ZAP-L) or a truncated form comprised only of the NTD (ZAP 254) to coimmunoprecipitate with TRIM25 was compared (**Figs 5C and S5B and S5C**). While full length ZAP and ZAP 254

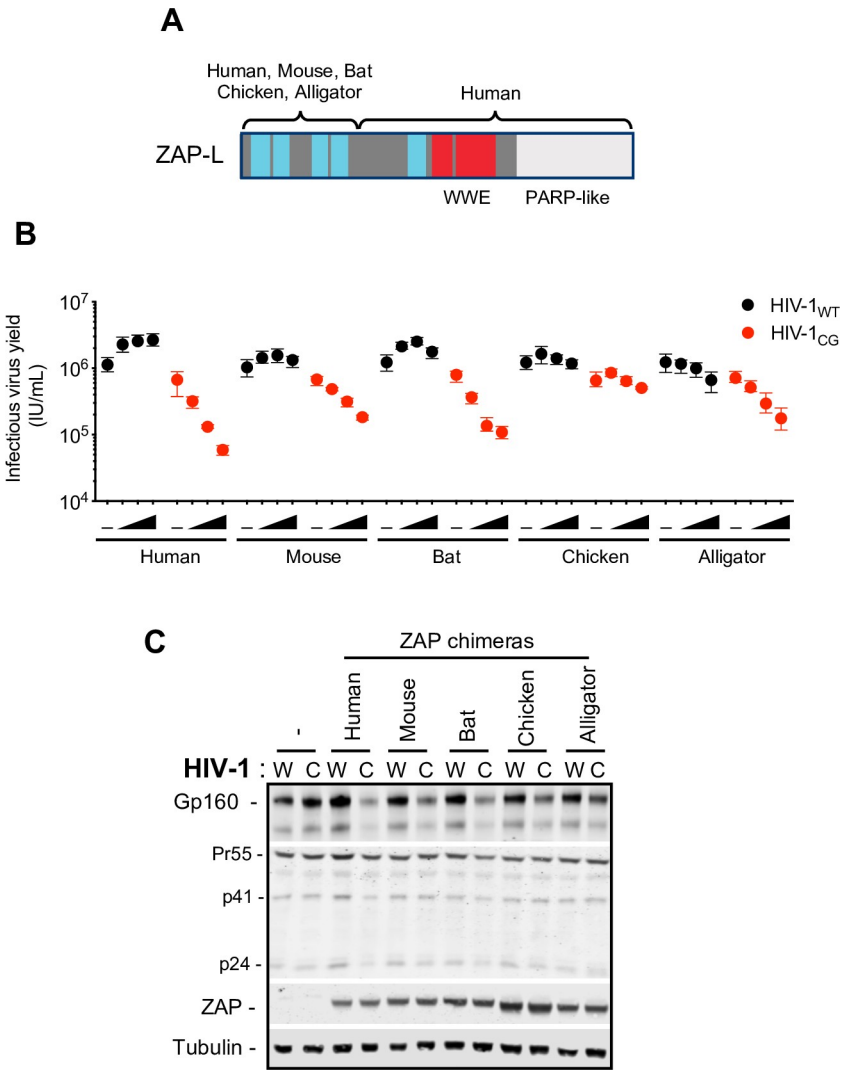

Fig 4. ZAP protein antiviral activity in human cells. (A) Schematic representation of ZAP chimeras in which the RNA binding domain of mouse, bat, chicken and alligator ZAP was fused to the WWE and PARP-like domain of human ZAP. (B-C) HEK293T ZAP$^{-/-}$ cells were transfected with HIV-1$_{WT}$ (W) or HIV-1$_{CG}$ (C) proviral plasmids and increasing amounts (0ng, 75ng, 145ng, or 290ng) of a plasmid encoding each ZAP chimera. Supernatant was harvested after 48h and the infectious virus yield was determined using MT4-R5-GFP target cells (B). Whole cell lysates corresponding to the highest amount of ZAP plasmids transfected were analysed by western blotting probing with antibodies against HIV-1 proteins and ZAP (C). -, Indicates co-transfection with an empty vector in place of a ZAP expression plasmid.

https://doi.org/10.1371/journal.ppat.1009545.g004

coimmunoprecipitated with TRIM25, the inactive (Fig 5D) truncated ZAP, lacking the NTD, failed to coimmunoprecipitate with TRIM25 (Fig 5C). These data suggest that ZAP and TRIM25 functionally interact via the N-terminal ZAP zinc finger domain and the C-terminal SPRY domain of TRIM25.

Since both the ZAP NTD and TRIM25 proteins can bind RNA [12,21,22], it was possible that RNA might have a bridging function and be responsible for the interaction between the two proteins. To explore this hypothesis, we generated a ZAP mutant (R74A, R75A, K76A, hereafter referred to as ZAP RNA^{null}). Notably ZAP RNA^{null} bound undetectable levels of RNA in crosslinking immunoprecipitation assays (Fig 5E). We transfected HEK293T ZAP$^{-/-}$

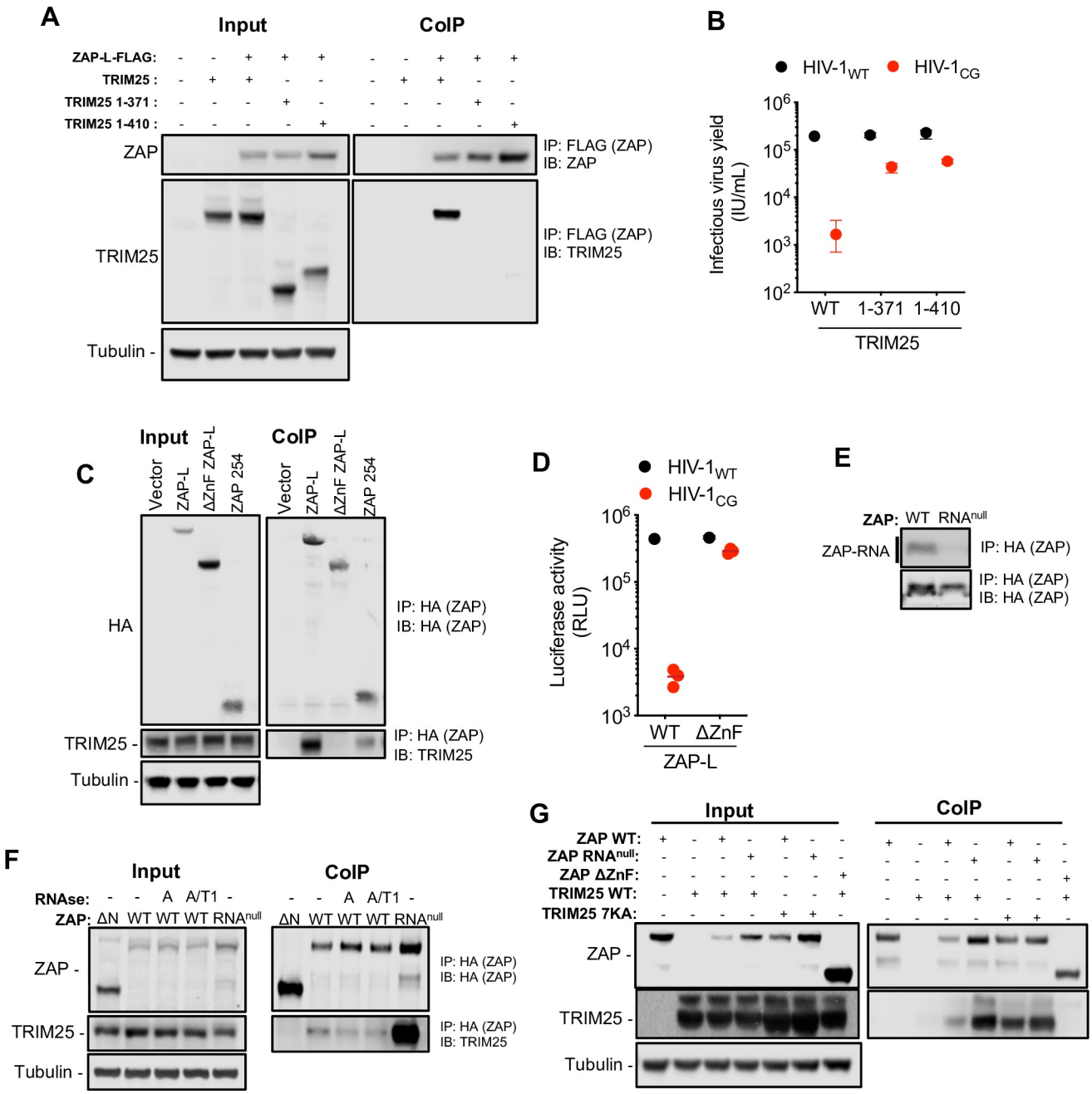

Fig 5. TRIM25 binds the ZAP NTD independently of RNA. (A) HEK293T ZAP$^{-/-}$ and TRIM25 $^{-/-}$ cells were co-transfected with plasmids expressing human ZAP-L-FLAG and full-length untagged human TRIM25 or one of two human TRIM25 truncations (corresponding to the N-terminal 371 or 410 amino acids of TRIM25), that lack the SPRY domain [21]. Proteins were immunoprecipitated from cell lysates with an anti-FLAG antibody and subjected to western blot analysis. IP, immunoprecipitation. IB, immunoblot. (B) HEK293T ZAP$^{-/-}$ TRIM25 $^{-/-}$ cells were co-transfected with proviral plasmids and plasmids encoding human ZAP and full-length TRIM25 or the indicated truncated TRIM25 proteins. Infectious virus yield was determined using MT4-R5-GFP target cells. (C) HEK293T ZAP$^{-/-}$ cells were transfected with an empty vector or plasmids encoding human ZAP-L-HA, a truncated ZAP lacking the RNA binding domain (ΔZnF ZAP-L) or a truncated ZAP comprising the N-terminal 254 amino acids (ZAP 254). Proteins were immunoprecipitated from cell lysates with an anti-HA antibody and analysed by western blotting to detect overexpressed ZAP-L-HA and endogenous TRIM25. (D) Antiviral activity of ΔZnF ZAP-L was assessed by co-transfecting HEK293T ZAP$^{-/-}$ cells with indicated proviral plasmids and plasmids encoding full length (WT) or truncated (ΔZnF) human ZAP. Infectious virus yield was determined using MT4-R5-GFP target cells. (E) HEK293T ZAP$^{-/-}$ cells were transfected with plasmids encoding human ZAP-L (WT) or an RNA-binding mutant of ZAP (RNA^{null}, R74A, R75A, K76A). After overnight incubation cells were irradiated with UV light, and ZAP proteins were immunoprecipitated. RNA bound to each protein was radiolabelled and protein-RNA adducts were resolved by SDS-PAGE, transferred to a nitrocellulose membrane and exposed to autoradiographic film. In parallel, a western blot of immunoprecipitated proteins was done using anti-HA antibody. IP, immunoprecipitation. IB, immunoblot. (F) HEK293T ZAP$^{-/-}$ cells were transfected

with plasmids encoding HA-tagged human ZAP-L (WT), ΔZnF ZAP-L or ZAP (RNA^{null}). Cell lysates were treated with RNAse A or a mixture of RNAse A and T1. ZAP protein complexes immunoprecipitated and subjected to western blot analysis to detect overexpressed ZAP-L-HA and endogenous TRIM25. (G) HEK293T $ZAP^{-/-}$ and $TRIM25^{-/-}$ cells were transfected with plasmids encoding HA-tagged ZAP-L (WT), ΔZnF ZAP-L or ZAP (RNA^{null}), along with untagged TRIM25 or a TRIM25 RNA binding mutant (TRIM25 7KA). ZAP-HA protein complexes immunoprecipitated and subjected to western blot analysis to detect overexpressed ZAP and TRIM25 proteins.

https://doi.org/10.1371/journal.ppat.1009545.g005

cells with plasmids expressing wildtype ZAP-L or the ZAP RNA^{null} mutant, lysed the cells and treated the cell lysates with RNase A or a mixture of RNase A and T1 prior immunoprecipitation (Fig 5F). RNase A or A/T1 treatment only slightly affected coimmunoprecipitation of ZAP with endogenous TRIM25. Furthermore, the ZAP RNA^{null} mutation increased, rather than decreased, the amounts of coprecipitated endogenous TRIM25. Similarly, in experiments where HEK293T $ZAP^{-/-}$ $TRIM25^{-/-}$ cells were cotransfected with plasmids expressing wildtype or RNA-binding-defective mutants of ZAP (ZAP WT and ZAP RNA^{null}) and TRIM25 (TRIM25 WT and TRIM25 7KA [21]), the amount of coprecipitated TRIM25 did not suggest a role for RNA in mediating ZAP-TRIM25 interactions (Fig 5G). Specifically, the amount of TRIM25 coprecipitated with ZAP was the same or increased when either ZAP RNA^{null} or TRIM25 7KA mutants were expressed in place of the wild-type proteins. Overall, these results suggest that ZAP NTD and TRIM25 interact in a manner that is dependent on protein-protein rather than protein-RNA interactions.

Since human TRIM25 interacted with human ZAP in an NTD dependent manner, but the ZAP chimeras encoded an NTD from a different species, it was possible that an inability to functionally interact with endogenous human TRIM25 was responsible for their absent or poor activity in some ZAP chimeras in human cells. To explore this hypothesis, we tested whether the expression of TRIM25 from various species could support the activity of ZAP chimeras encoding a ZAP NTD from that species. TRIM25-related genes are present in mammals, birds and reptiles and some species of fish (Fig 6A). To assess whether the expression of cognate TRIM25 could augment the antiviral activity of each ZAP chimera, we measured infectious $HIV\text{-}1_{CG}$ yield from HEK293T $ZAP^{-/-}$ $TRIM25^{-/-}$ cells cotransfected with plasmids expressing TRIM25 and chimeric ZAP proteins from various species (**Figs 6B and S6A and S6B**). While there was some variation in potency, ZAP chimeras from mammalian species generally exhibited antiviral activity in the presence of TRIM25, regardless of the species of origin. Conversely ZAP proteins from more distantly related species (chicken and alligator) were poorly active when coexpressed with mammalian TRIM25 proteins, but exhibited greater antiviral activity when coexpressed with a TRIM25 protein from the same species (Fig 6B). Of note, expression of cognate TRIM25 slightly affected the expression of each ZAP chimera (S6C Fig), perhaps through ZAP ubiquitination reactions [7,22].

To test whether the ZAP NTD from the various species had the same or different target RNA specificities, HEK293T $ZAP^{-/-}$ and $TRIM25^{-/-}$ were co-transfected with plasmids expressing a ZAP chimera and a cognate TRIM25 protein, together with a $HIV\text{-}1_{WT}$ or $HIV\text{-}1_{CG}$ proviral plasmid (Fig 7A and 7B). Interestingly, while all the ZAP/TRIM25 proteins reduced the yield of $HIV\text{-}1_{CG}$, some of the TRIM25 and ZAP chimera combinations also reduced the yield of $HIV\text{-}1_{WT}$ to some extent. This was particularly the case for the chicken TRIM25 and ZAP chimera combination which reduced the yield of infectious $HIV\text{-}1_{WT}$ by >10 fold at the highest dose tested, suggesting that ZAP from chicken might have a different or expanded RNA binding specificity.

Birds comprise one of the most diverse phyla in vertebrates, with about 10,000 species, adapted to a wide range of habitats [23]. Since chicken ZAP was phenotypically distinct from other vertebrate ZAPs, we investigated whether ZAP from other species of birds share a similar phenotype with chicken ZAP. We constructed chimeric ZAP proteins in which the RNA

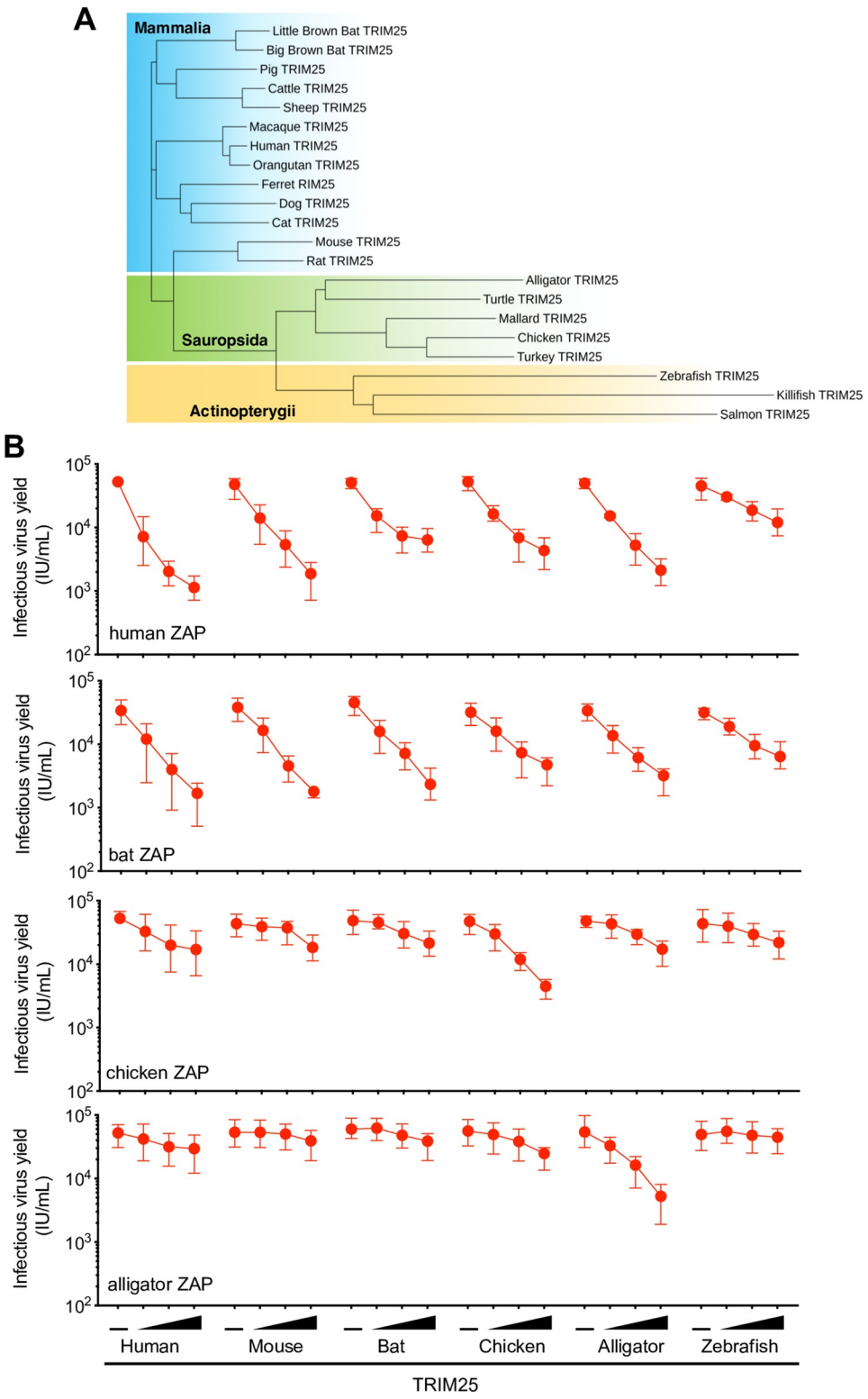

Fig 6. ZAP proteins from tetrapods have antiviral activity in the presence of cognate TRIM25. (A) Phylogenetic analysis of TRIM25 protein sequences from vertebrate species. Shaded areas indicate cluster sequences from mammals (in blue), birds and reptiles (in green) and ray-finned fish (in yellow). (B) HEK293T ZAP$^{-/-}$ and TRIM25$^{-/-}$ cells were co-transfected with an HIV-1_{CG} proviral plasmid as well as a fixed amount of a plasmid encoding human ZAP or ZAP chimeras from various vertebrate species. Animal names indicate source of the RNA-binding domains for each ZAP

chimera. For each ZAP protein, cells were also co-transfected increasing amounts of a plasmid (0ng 10ng, 30ng or 90ng) expressing a TRIM25 protein from the 6 different indicated species. After 48h, infectious virus yield was determined using MT4-R5-GFP target cells.

https://doi.org/10.1371/journal.ppat.1009545.g006

binding domain was from one of several additional bird species: three from the order *Galliformes*–chicken (*Gallus gallus*), turkey (*Meleagris gallopavo*) and duck (*Anas platyrhynchos*)–and two from the suborder *Neoaves*–eagle (*Aquila chrysaetos canadensis*) and zebra finch

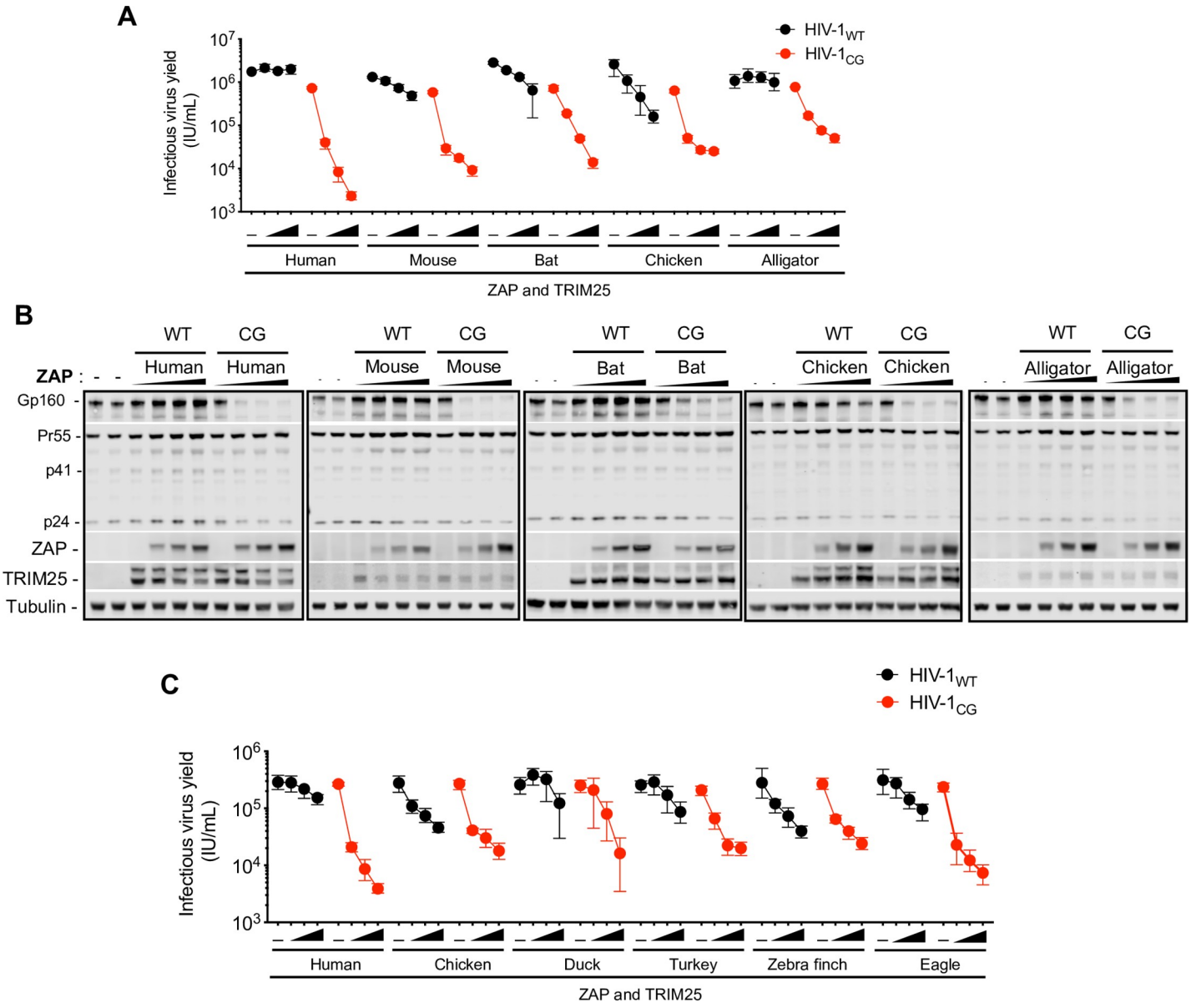

Fig 7. Avian ZAP proteins are less selective for CpG enriched HIV-1. (A-B) HEK293T ZAP$^{-/-}$ and TRIM25$^{-/-}$ cells were co-transfected with indicated proviral plasmids, increasing amounts (0ng, 75ng, 145ng, or 290ng) of a plasmid encoding an FLAG-tagged human ZAP or mouse, bat, chicken and alligator ZAP chimeras and a fixed amount of a plasmid encoding a cognate HA-TRIM25 protein. After 48h, infectious virus yield was determined using MT4-R5-GFP target cells (A). Whole cell lysates were analysed by western blotting probing with antibodies against HIV-1 proteins ZAP-FLAG and TRIM25-HA (B). (C) HEK293T ZAP$^{-/-}$ and TRIM25$^{-/-}$ cells were transfected with HIV-1 proviral plasmids, along with increasing amounts (0ng, 75ng, 145ng, or 290ng) of a plasmids expressing human ZAP or ZAP chimeras from various avian species. For cells transfected with human ZAP, a fixed amount of a human TRIM25 expression plasmid was co-transfected, while for the avian ZAP chimeras, chicken TRIM25 was used. After 48h, infectious virus yield was determined using MT4-R5-GFP target cells.

https://doi.org/10.1371/journal.ppat.1009545.g007

(*Taeniopygia guttata*) (**Figs 7C and S6D**). The avian ZAP chimeric proteins exhibited different levels of antiviral activity, but some, particularly the chicken and zebra finch ZAP chimeras reduced HIV-1_{WT} yield (**Figs 7C and S6D**). Indeed, the zebra finch ZAP chimera was nearly as potent against HIV-1_{WT} as it was against HIV-1_{CG}. All avian ZAP chimeras were detected at similar levels by western blot analysis, with the exception of the duck ZAP chimera that was expressed at lower levels. These findings suggest that a loss of selectivity for CpG-rich RNA, or expansion of RNA target specificity has occurred on more than one occasion in avian ZAP proteins.

RNA-binding specificity of chicken and human ZAP proteins differs

Since human ZAP binds to CG-rich RNA with high selectivity [11,12], differences in RNA binding affinity and specificity might explain the altered antiviral specificity of some avian ZAP proteins. We focused on chicken ZAP, and used crosslinking immunoprecipitation coupled with RNA sequencing (CLIP-Seq) to determine its RNA-binding preference in HEK293T $ZAP^{-/-}$ $TRIM25^{-/-}$ cells cotransfected with an HIV-1_{CG} proviral plasmid along with plasmids encoding human or chicken ZAP. This analysis revealed that, as expected and previously reported [11], human ZAP bound primarily to regions of the genome that contained a high number of CpG dinucleotides (**Fig 8A**), Notably, the chicken chimeric ZAP preferentially bound to the CpG-rich portion of the viral genome, but also exhibited a comparatively higher level of binding to the CpG-poor portions of the viral genome. We quantified the representation of each of the 16 dinucleotides in ZAP-crosslinked total reads from the viral genome for both human and chicken ZAP (**Fig 8B**). While CpG dinucleotides were enriched in RNAs crosslinked to both chicken and human ZAP chimeras, CpG enrichment was clearly less pronounced in chicken ZAP. The reduced specificity of chicken ZAP for HIV-1_{CG} was mirrored in experiments where by the overexpression of either human ZAP or chicken ZAP chimera were coexpressed with luciferase-based reporters containing as 3' UTR VSV-derived sequences with low (WT) or high (CG) CpG dinucleotide frequencies (**S7A Fig**). Indeed, while human ZAP reduced luciferase activity only when a CG-rich 3' UTR was present, the chicken ZAP chimera reduced the activity of both luciferase reporters. Together these data suggest that chicken ZAP is less selective toward CpG-rich RNA and this property corelates with the broader antiviral activity of chicken ZAP.

A determinant in the ZAP NTD that governs species-specific TRIM25 dependence

The maximal antiviral activity of the chicken ZAP NTD chimera requires chicken TRIM25. In an attempt to determine what region in the ZAP NTD is responsible for this species-specific dependence, we inspected aligned protein sequences from human and chicken ZAP NTDs. We noticed that a divergent protein sequence, composed of two predicted α-helices is present in the C-terminal portion of the NTD (**Figs 9A, 9B, and S8**). Based on the crystal structure of human ZAP [12], these α-helices are located proximal to the third and fourth zinc fingers, facing away from the RNA-binding pocket (**Fig 9A**). To test whether this element is important for species-specific TRIM25 dependence, we generated a chimera that contained the four N-terminal zinc fingers from chicken ZAP, and the divergent NTD α-helices from the human ZAP (chZAP-X, **Fig 9B**). We compared the activity of chZAP-X with that of the human ZAP, and the previously constructed chZAP chimera in the presence of human or chicken TRIM25 (**Fig 9C**). As previously observed, human ZAP was active against HIV-1_{CG} in the presence of either human or chicken TRIM25. Conversely, the original chZAP chimera was more potent in the presence of chicken TRIM25 than human TRIM25, and also exhibited activity against

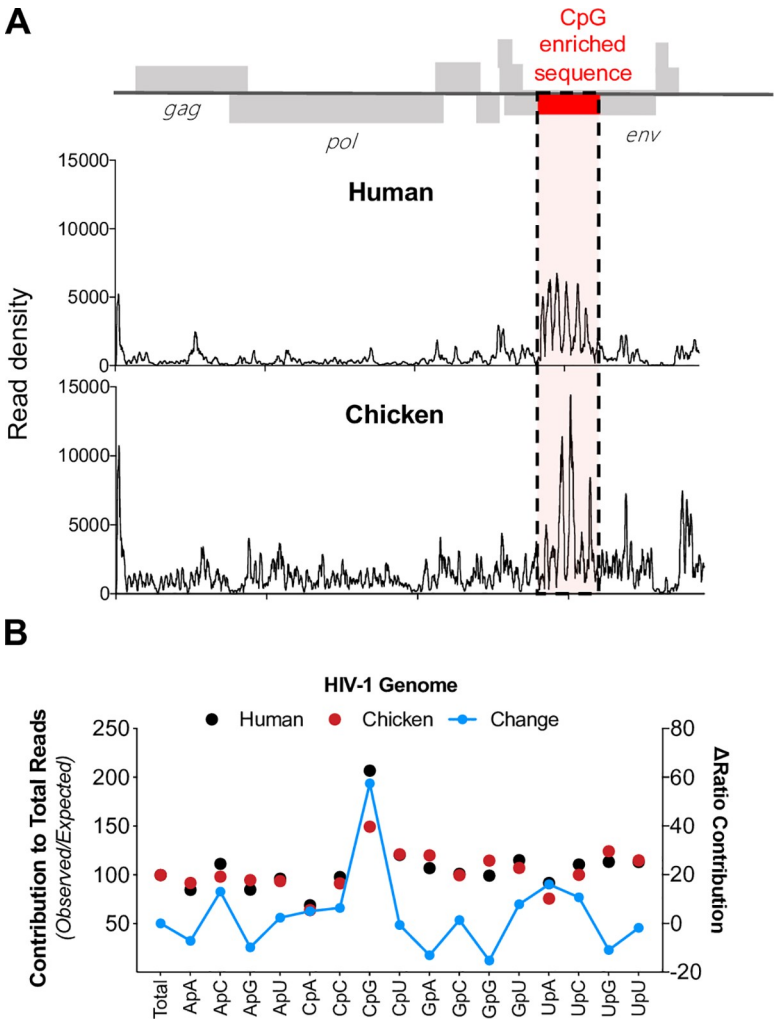

Fig 8. Differences in the RNA binding profiles of human and chicken ZAP. (A) HEK293T ZAP$^{-/-}$ and TRIM25$^{-/-}$ cells were transfected with an HIV-1_{CG} proviral plasmid and a plasmid expressing human ZAP or chicken ZAP chimera. Cells were treated with 4-thiouiridine prior to UV-crosslinking and CLIP analysis. Reads associated with human (top) or chicken (bottom) ZAP were mapped to the HIV-1_{CG} genome and the read density plotted against position in the HIV-1_{CG} genome. CpG-enriched region the HIV-1_{CG} genome is highlighted in red and dashed lines. (B) Contribution (% observed/expected) for each dinucleotide to reads derived from the HIV-1_{CG} genome to was calculated. Shift in the ratio for each dinucleotide contribution comparing human and chicken ZAP reads was also determined (blue line).

https://doi.org/10.1371/journal.ppat.1009545.g008

HIV-1_{WT} in the presence of chicken TRIM25 (Fig 9C). Notably, the ZAP-X chimera was more active against HIV-1_{CG} than chZAP in the presence of human TRIM25. Moreover, chZAP-X was also active against HIV-1_{WT} in the presence of either human or chicken TRIM25. Overall these data indicated that the four NTD zinc fingers of chicken ZAP are responsible for the its expanded antiviral activity against HIV-1_{WT}, while the two divergent NTD α-helices are at least partly responsible for the species-specific dependence of chicken ZAP protein on chicken TRIM25.

Discussion

The emergence of genes with new functions is central to the adaptability of organisms to new challenges. Viral infections impose a strong selective pressure on their hosts, thus gene

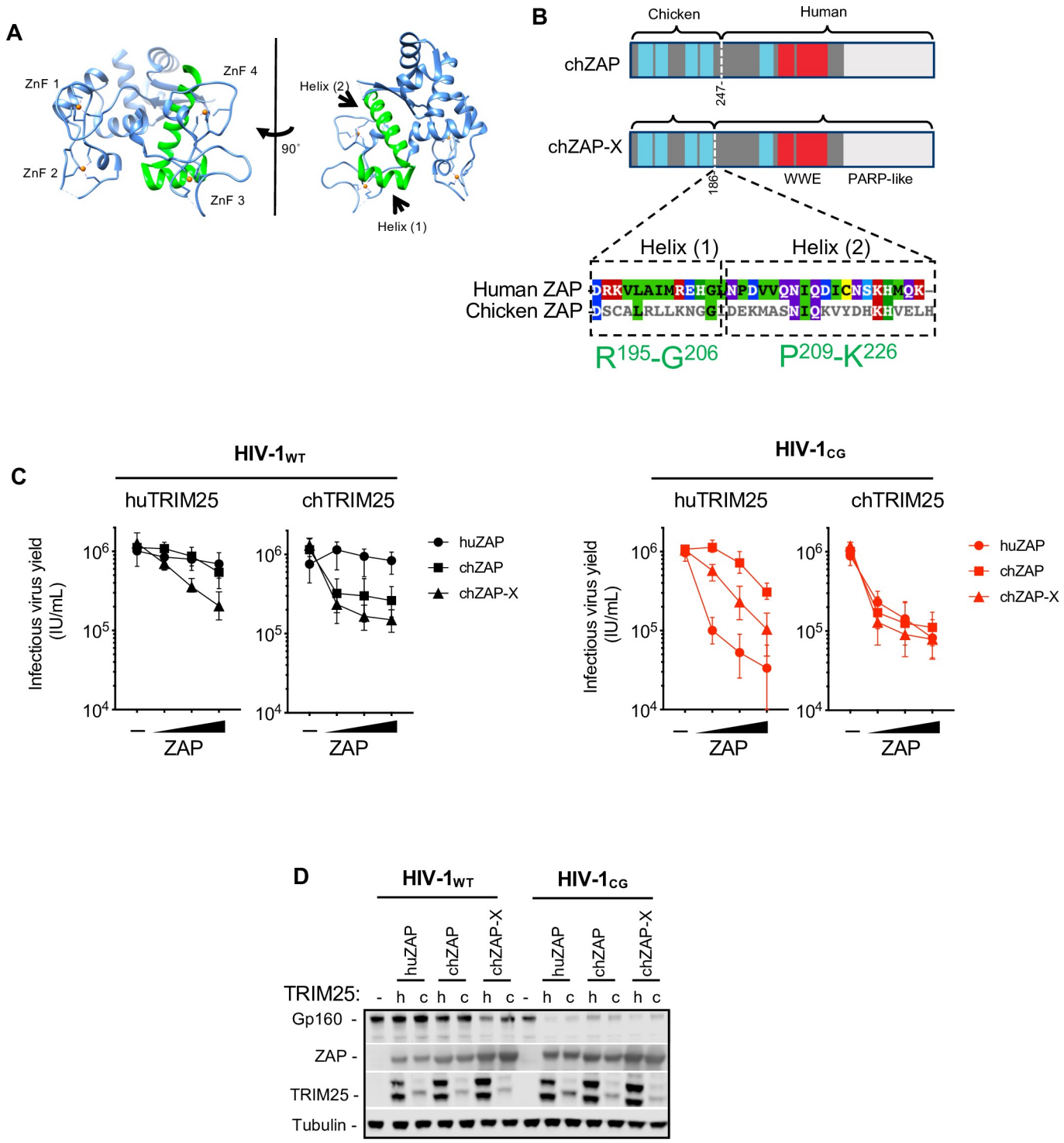

Fig 9. A determinant in the ZAP NTD contributes to the species-specific cognate TRIM25 requirement. (A) Representation of the crystal structure of the RNA-binding NTD domain of human ZAP (PDB 6UEI, [12]). ZnF 1–4 indicate zinc fingers 1 through 4. Areas colored in green indicate α-helices 1 and 2 at the C-terminus of the NTD. (B, top) Schematic diagram of chicken ZAP (chZAP) chimera, containing the N-terminal 247 amino acids of chicken ZAP, in an otherwise human ZAP background, and chicken ZAP-X (chZAP-X) chimera, that contains the N-terminal 186 amino acids of chicken ZAP in a human ZAP background. chZAP-X contains the two human α-helices highlighted (A). (B, bottom) Sequence alignment of the α-helices 1 and 2 in human ZAP with the corresponding region in chicken ZAP. Colors indicate amino acid identity and conservation. The position numbers for the two α-helices in humanZAP are indicated in green. (C-D) HEK293T ZAP$^{-/-}$ and TRIM25$^{-/-}$ cells were co-transfected with HIV-1_{WT} and HIV-1_{CG} proviral plasmids, as well as plasmids encoding human ZAP (huZAP), chicken ZAP chimera (chZAP) and the chicken ZAP-X (chZAP-X) chimera and either human TRIM25 or chicken TRIM25. After 48h,

infectious virus yield was determined using MT4-R5-GFP target cells (C). Whole cell lysates were analysed by western blotting probing with antibodies against HIV-1 proteins ZAP-FLAG and TRIM25-HA (D).

https://doi.org/10.1371/journal.ppat.1009545.g009

products with antiviral functions constitute prominent examples of genetic innovation and are among the fastest evolving genes [24]. While our analysis suggests that *ZAP* originated from a duplication of the *PARP12* gene, and both human PARP12 and ZAP have been reported to exert antiviral activity against a broad range of viruses, the mechanisms by which they exert their function are different. Specifically, ZAP proteins' antiviral function is primarily related to their RNA recognition [4,5,11], while PARP12 showed no detectable RNA-binding activity. Indeed previous work has indicated that PARP12 antiviral activity is linked to PARP domain-dependent ADP-ribosylation of viral proteins [17,25]. The PARP-like domain of mammalian ZAP proteins is catalytically inactive, and therefore, cannot catalyze ADP-ribosylation of viral or endogenous proteins [26,27]. Interestingly, however, sequence alignments of PARP domains of chicken and alligator ZAP revealed that these ZAP proteins likely contain catalytically active PARPs, raising the possibility that these are bifunctional antiviral proteins. A more recent gene duplication has apparently occurred in mammals, as revealed by the existence of another paralogue of ZAP, termed ZAP-like or *ZC3HAV1L*. This gene encodes a shorter protein, that contains four CCCH-type zinc fingers and appears paralogous to the ZAP RNA-binding domain (**S1 Fig**). Since the ZAP RNA-binding domain is sufficient to inhibit virus replication [4], it is plausible that ZC3HAV1L has antiviral activity. However, this awaits definitive experimentation.

Our prior work suggests that ZAP exploits the CpG suppressed state of human genomes to discriminate between self and non-self RNA [11]. CpG suppression in animal genomes is thought to be the by-product of DNA methylation and subsequent deamination of 5-methylcytosine into thymidine, followed by the repair of the mispaired G on the opposing strand [14]. Thus, the extent to which CpG dinucleotides in a given genome is methylated is linked to the degree of CpG suppression therein. Indeed, while the dinucleotide frequency distributions are similar for most dinucleotides in most organisms, CpG dinucleotide frequency in animal genomes can vary widely (**Fig 3A**). In particular, the coding sequences of several vertebrates (mammals, birds, reptiles, fish) and some non-arthropod invertebrates (molluscs) show substantial levels of CpG suppression, while in arthropods, nematodes and some species of plants the frequency of CpG dinucleotides is higher. This property correlates with the extent of DNA methylation observed in these organisms [28]. Thus, the CpG suppressed state of animal genomes creates the opportunity for self-nonself discrimination by ZAP-related proteins that has apparently been exploited in tetrapods. Nevertheless, one study showed the rate of CpG DNA methylation in genomes may be insufficient to explain the extent to which vertebrate mRNA is CpG-suppressed [29]. Indeed, RNA transcripts in some organisms seem to be under additional selective pressures to purge CpG dinucleotides, as suggested by the observed frequency of C-to-A mutations in a CpG context. Thus, it is possible that the emergence of ZAP/PARP12 related genes may have further shaped the dinucleotide composition of coding sequences in modern genomes.

We found that the activity of ZAP proteins from different organisms was inherently dependent on the cellular context. Indeed, in line with previous reports [7,8] we found that the expression of a ZAP cofactor, TRIM25, was important for its antiviral activity against CpG-enriched HIV-1. In fact, the activity of ZAP proteins from certain species (chicken and alligator) was dependent on the coexpression of a cognate TRIM25 protein. This species-specific dependency suggests that ZAP and TRIM25 interact in a way that is maintained across different species. Concordantly, replacing two poorly conserved α-helices immediately C-terminal

to the RNA binding domain in chicken ZAP with the equivalent element from human ZAP enabled the chimeric protein to function better in the presence of human TRIM25. This result strongly suggests a species-specific component of the interaction between ZAP and TRIM25. Consistent with this finding, prior work, confirmed herein, has suggested a physical interaction between ZAP and TRIM25 in a manner that was dependent on the TRIM25 SPRY domain [7]. Additionally, we showed that the ZAP NTD, that includes the RNA binding domain, is necessary and sufficient to co-immunoprecipitate TRIM25. Notably, two domains in TRIM25 have been reported to bind RNA: (1) a short section of positively-charged amino acids located between the coiled-coil domain and the PRY/SPRY domain (N-KKVSKEEKKSKK-C, amino acids 381–391 [21]), and (2) a small region (470–508) within the PRY/SPRY domain [22]). Additionally, two reports suggested that RNA enhances the E3-ubiquitin ligase activity of TRIM25 *in vitro* [21,22]. However, we found that a TRIM25 mutant in which the lysine cluster at 381–391 was replaced by alanines (TRIM25 7KA) supported antiviral activity. Moreover, TRIM25 7KA, ZAP-RNA^{Null} and RNAseA/T1 treatment were all compatible with ZAP-TRIM25 coprecipitation. Together, these results suggest that ZAP-TRIM25 interaction is not RNA-dependent and is likely mediated by protein-protein contacts. That there exists a species-specific restriction in ZAP-TRIM25 functional compatibility, that can be mapped to a specific protein element, is consistent with this notion.

Finally, we found that avian ZAP proteins, unlike human ZAP, exhibit varying degrees of antiviral activity against HIV-1_{WT} as well as HIV-1_{CG}. Consistent with this finding, CLIP-Seq analysis using chicken ZAP revealed that it binds more promiscuously throughout the viral genome than does human ZAP. Recently, two structures of ZAP (from human and mouse) bound to a target RNA elucidated the nature of the interaction between ZAP and CpG dinucleotides [12,13]. Key contacts are established by ZAP residues K89, Y98, K107 and Y108 [12]. Of these, K89, K107 and Y108 are conserved between human and chicken ZAP. Notably, the second zinc finger of chicken ZAP is three-amino acids shorter than the human counterpart; how the structural divergence between these human and avian ZAP influences RNA-binding specificity required further investigation, but mutations at various positions surrounding the CpG binding pocket in human ZAP can cause relaxation in strict CpG specificity [12]. An important caveat to these studies is that the ZAP constructs used herein are of chimeric nature, and therefore further investigation is required to validate the RNA-binding specificity of avian ZAP in their native cellular context. Interestingly, birds are important vectors for certain human viral infections, such as influenza and West Nile virus. The CpG dinucleotide content of influenza A viruses has progressively decreased in human populations following zoonotic transmission from birds [30,31]. Moreover, the frequency of CpG dinucleotides in viral genomes can be used to predict animal reservoirs [32]. In the case of birds, viruses that infect *Neoaves*–and to some extent viruses that infect *Galliformes*–have higher CpG dinucleotide frequencies than viruses that infect primates or rodents. Together, our results provide a potential molecular explanation for the observed fluctuations in CpG-content of viruses that have adapted to different hosts, and suggest that ZAP's antiviral activity represents a selective pressure that influences the dinucleotide composition of viral genomes.

Overall, these findings highlight the potential for innovation of gene function driven by viral infection. Understanding how different organisms have evolved to control infections will illuminate the mechanisms of host range restriction and enable novel interventions in viral diseases.

Materials and methods

Cells

Human embryonic kidney (HEK) 293T, HEK293T ZAP$^{-/-}$ [11], HEK293T ZAP$^{-/-}$ TRIM25$^{-/-}$ [7] and chicken fibroblasts DF1 (ATCC, CRL-12203) were cultured in Dulbecco's Modified

Eagle's Medium (DMEM) supplemented with foetal bovine serum (FBS). *Eptesicus fuscus* kidney (EFK) cells were purchased from Kerafast, Inc (ESA001) and cultured in DMEM supplemented with FBS. Mouse embryonic fibroblasts (MEFs, [33]) were cultured in DMEM supplemented with bovine calf serum (BCS). MT4-R5-GFP cells [34] were grown in RPMI medium supplemented with FBS. All cells were maintained at 37˚C in 5% CO_2.

Plasmids

Sequences encoding the RNA-binding domains of alligator, turkey, duck, zebra finch and eagle ZAP were retrieved from the NCBI nucleotide database and DNA was synthesised by Twist Biosciences. Total RNA from EFK cells was extracted using the NucleoSpin RNA purification kit (Macherey-Nagel) according to manufacturer's guidelines, reverse transcribed into cDNA using the SuperScript III First-Strand Synthesis System (Invitrogen), and bat ZAP was amplified using specific primers. TRIM25 mRNA was isolated from MEF, EFK, DF1 cell lines, as above, and reverse transcribed to generate cDNA. Alligator, turkey, duck, zebra finch and eagle TRIM25 cDNA was synthesised by Twist Biosciences. Total RNA from the intestine of a zebrafish specimen (kindly provided by Professor A. James Hudspeth, The Rockefeller University) was extracted and TRIM25 cDNA was generated as before. ZAP chimeras were generated by fusing the RNA-binding domain of ZAP isolated from indicated species to the residues 255–902 of the long isoform of human ZAP-L, that was C-terminally tagged with three HA epitopes or one FLAG epitope, as indicated, and inserted into the expression plasmid pCR3.1. TRIM25 sequences were fused to a C-terminal HA epitope and inserted into pCR3.1. The two truncated versions of TRIM25 (1–371 and 1–410) and the TRIM25 7KA mutants were a kind gift from Owen Pornillos, University of Virginia [21]. The ZAP RNA^{null} mutant was generated by introducing three point-mutations R74A, R75A and K76A by overlap extension PCR.

Bioinformatics

The protein sequences of human ZAP and PARP12 were retrieved from GeneBank. These sequences were subsequently used to identify orthologues in other species using the Blastp suite of NCBI. Sequences with significant E-values were used for subsequent sequence alignments and phylogenetic analysis. We considered the identified protein sequences to be products of orthologues of *ZC3HAV1*/*PARP12* if (1) significant sequence homology was observed, (2) if sequences contained 5 CCCH-type zinc fingers and (3) if WWE and PARP-like domains were present. MUSCLE was used to perform multiple sequence analysis. Phylogenetic trees were derived using BEAST [35] and plotted using FigTree. Speciation dates were based on [36]. A similar approach was taken to identify and analyse *TRIM25* orthologues. For synteny studies, *ZC3HAV1*/*PARP12* loci from different vertebrate species were analysed using Ensembl and Genomicus Browsers.

For nucleotide composition studies, RNA transcript sequences from human (*Homo sapiens*), house mouse (*Mus musculus*), little brown bat (*Myotis lucifugus*), chicken (*Gallus gallus*), alligator (*Alligator mississippiensis*), dog (*Canis familiaris*), zebrafish (*Danio rerio*), California two-spot octopus (*Octopus bimaculoides*), oyster *(Crassostrea gigas)*, mosquito (*Aedes aegypti*), sandfly (*Lutzomyia longipalpis*), tick (*Ixodes scapularis*), pacific white shrimp (*Litopenaeus vannamei*), *Caenorhabditis elegans*, coral (*Acropora digitifera*) and *Arabidopsis thaliana* were retrieved from the NCBI nucleotide sequence database. Subsequently, sequences were fragmented into 5' UTRs, ORFs and 3'UTRs. Mononucleotide and dinucleotide frequencies were calculated using the SSE suite [37] and analysed using in-house R scripts.

Virus yield assays

To assess the activity of different zinc finger proteins, virus yield was measured as described previously [12]. In brief, HEK293T $ZAP^{-/-}$ $TRIM25^{-/-}$ were seeded onto a 24-well plate and transfected with 375ng of HIV-1_{WT} or HIV-1_{CG} proviral plasmids, along with 87ng of a plasmid encoding TRIM25 and varying amount of ZAP expression constructs, unless otherwise indicated. After 24h, media were replaced and at 48h post-transfection supernatants were collected, filtered through a 0.22μm filter and titres determined using MT4-R5-GFP target cells. Transfected cells were lysed in NuPAGE buffer and protein samples were analysed by western blotting.

Luciferase assays

Expression constructs encoding a recoded, low-CpG firefly luciferase and containing wildtype or CpG-enriched VSV-G or IAV-NP sequences as 3' UTRs were used to assess the activity of ZAP and PARP12, as described before [11]. Cells were co-transfected with 50ng of luciferase-encoding plasmids, 250ng of plasmids encoding human ZAP-L or PARP12 and human TRIM25. After 56h, cells were lysed in cell lysis buffer and luciferase activity was measured using the Luciferase Assay System (Promega).

Western blotting

Cell lysates were incubated at 72˚C for 20min and sonicated for 20s. Protein samples were resolved in a 4–12% PAGE gel (Novex) using MOPS running buffer. Protein was transferred to a nitrocellulose membrane, blocked at room temperature and incubated with the following antibodies: anti-ZC3HAV1 (rabbit, 1:10,000, clone 16820-1-AP, Proteintech Group), anti-TRIM25, anti-HA (rabbit, 1:5000, clone 600-401-384, Rockland), anti-Tubulin (mouse, 1:10,000, clone DM1A T9026, Millipore-Sigma), anti-HIV-1 Env (goat, 1:1000, 12-6205-1, American Research Products). Blots were washed and incubated with secondary antibodies: anti-Mouse IgG IR700 Dye Conjugated (Licor), Anti-Rabbit IgG IR800 Dye conjugated (Licor), Anti-Goat IgG IR800 Dye Conjugated (Licor) and Anti-Rabbit IgG horseradish peroxidase conjugated (Jackson). Blots were imaged immediately in a Licor Odyssey scanner or incubated with ECL substrate and imaged on a CDigit blot scanner.

RNA-protein immunoprecipitation

Cells were seeded onto a 15cm dish and transfected, 24h later, with 8μg of plasmids encoding ZAP-L-3xHA, PARP12-3xHA or ZAP RNA^{Null} (R74A,R75A, K76A)-3xHA. The following day, media were replaced by culture media containing 4-thiouridine. Two days after transfection, cells were exposed to UVB light (0.15 J $cm^{-2,}$ λ = 365 nm, Stratalinker 2400 UV), washed in PBS and lysed in Lysis Buffer (10mM HEPES pH7.5, 30mM KCl, 40μM EDTA, 0.1% Igepal CA-630 supplemented with protease inhibitor cocktails). Lysates were clarified by centrifugation and incubated with RNAse A for 5min at 37˚C. Anti-HA mouse antibody (BioLegend) was adsorbed to protein G agarose beads and incubated with the cell lysates for 2h at 4˚C. Beads were washed twice in NP40 Lysis Buffer, twice IP wash buffer (50mM HEPES pH 7.5, 300mM KCl, 2mM EDTA, 0.5% Igepal CA-630), twice in LiCl buffer (250mM LiCl, 10mM Tris pH 8.0, 1mM EDTA, 0.5% Igepal CA-630, 0.5% sodium deoxycolate), twice in NaCl Buffer (50mM Tris pH 7.5, 1M NaCL, 1mM EDTA, 0.1 SDS, 0.5% sodium deoxycholate) and twice in KCl buffer (50mM HEPES pH 7.5, 500 mM KCl, 0.05% Igepal CA-630). RNA:Protein complexes were incubated with calf intestinal phosphatase (NEB) for 13min at 37˚C and washed in phosphatase wash buffer (50mM Tris HCl pH 7.5, 20mM EGTA, 0.5% NP40).

Beads were resuspended in PNK buffer (50 mM Tris HCl pH 7.5, 50mM NaCl, 10mM $MgCl_2$) and incubated with 5 U of PNK in the presence of 0.5 μCi/μL γ-^{32}P ATP. Beads were washed, lysed in NuPAGE Lysis buffer and RNA:Protein complexes were resolved in a 4–12% NuPAGE gel. Complexes were transferred to nitrocellulose membrane and exposed to autoradiographic film.

Co-immunoprecipitation

To evaluate ZAP and TRIM25 interactions, cells (HEK293T ZAP$^{-/-}$ or HEK293T ZAP$^{-/-}$ TRIM25$^{-/-}$) were seeded onto a 10cm dish and co-transfected, 24h later, with 3μg of a plasmid encoding ZAP-FLAG and 3μg of a plasmid encoding TRIM25-3xHA. In experiments in which endogenous TRIM25-positive cells were transfected, only ZAP-encoding plasmids were used. Cells were lysed 48h after transfection in 1.5mL of Lysis Buffer (10mM HEPES pH7.5, 30mM KCl, 40μM EDTA, 0.1% Igepal CA-630 supplemented with protease inhibitor cocktails). Lysates were clarified by centrifugation and treated with RNAse A (Roche, 100 Units) or RNAse A/T1 (NEB, 100 Units) for 5min at 37˚C. Protein G agorose beads that were pre-adsorbed to either anti-HA (BioLegend) or anti-FLAG (Millipore) antibodies were added to the lysates and incubated at 4˚C for 2h. Magnetic beads were captured and washed twice in lysis buffer and three times in IP wash buffer (50mM HEPES pH 7.5, 300mM KCl, 2mM EDTA, 0.5% Igepal CA-630). Protein complexes were resuspended in NuPAGE buffer and resolved on a 4–12% PAGE gel, transferred to nitrocellulose membranes and analysed by western blotting.

CLIP-Seq

RNA:protein complexes were isolated as described above. RNA was isolated and prepared for sequencing as before [38]. In brief, after isolation of RNA:protein complexes, RNA was released using Proteinase K (Roche). Purified RNA fragments were ligated to 3' and 5' adaptors, reverse transcribed (SuperScript First-Strand cDNA Synthesis System, Invitrogen) and amplified by PCR. The resulting cDNA library was sequenced using the Illumina HiSeq 2000 platform. Sequencing reads were processed and analysed as described previously [11].

Supporting information

S1 Fig. Homology among ZAP, PARP12 and ZAP-like proteins. (A) Protein sequence alignment of the N-terminal domain (NTDs) of human ZAP, PARP12 and ZAP-like protein. Colored residues indicate amino acid properties and conservation. (B) Percentage identity matrix among human ZAP, PARP12 and ZAP-like proteins. (C) Locus surrounding human *ZAP* and *ZAP*-like genes in chromosome 7. (D) Percentage protein similarity one-to-one matrix among ZAP and PARP12 paralogues found in vertebrate and invertebrates species. Hs, *Homo sapiens* (human); Mm, *Mus musculus* (mouse); Ml, *Myotis lucifugus* (little brown bat), Gg, *Gallus gallus* (chicken); Am, *Alligator mississipiensis* (alligator); Dr, *Danio rerio* (zebrafish); Lc, *Latimeria chalumnae* (Coelacanth); Ob, *Octopus bimaculoides* (California two-spot octopus); Cg, *Crassostrea gigas* (oyster); Ad, *Acropora digitifera* (coral).
(TIF)

S2 Fig. Evolution of *ZAP/PARP12*-related genes in teleost fish. (A) Phylogenetic analysis of ZAP and PARP12-related sequences found in the genomes of tetrapods and teleost fish. Blue box marks cluster of sequences unique to teleost fish. (B) Schematic representation of the domain organization of human ZAP and zebrafish PARP12a, PARP12b and ZC3HD1CL. (C) Diagram of the proposed evolution of *ZAP/PARP12*-related genes in tetrapods and teleost fish.

MYA, million years ago.
(TIF)

S3 Fig. Dinucleotide composition in mRNA 3'UTRs across vertebrates. (A) The 3' untranslated regions of mRNA transcripts found in transcriptomes of several vertebrates were collected from the NCBI nucleotide database and dinucleotide frequency ratio (observed/expected) was calculated and frequency distribution for each dinucleotide was plotted.
(TIF)

S4 Fig. Expression of wildtype and ZAP chimeras from different tetrapods. (A) HEK293T $ZAP^{-/-}$ cells were transfected with plasmids encoding wildtype or chimera ZAP from human (H), mouse (M), bat (B), chicken (C) or alligator (A). As a control, cells were transfected with an equivalent amount of an empty plasmid (-). After 48h, whole cell lysates were generated and analysed by SDS-PAGE/western blot. (B) HOS $ZAP^{-/-}$ cells were transduced with vectors encoding human ZAP or ZAP chimeras all C-terminally tagged with the HA epitope. Expression of ZAP was induced by treatment with doxycycline and 48h later cells were fixed, stained with an anti-HA antibody and immunofluorescent antibodies and imaged. Micrographs are representative of each imaged condition.
(TIF)

S5 Fig. Domains of ZAP required for its antiviral activity. (A) Western blot analysis of HEK293T and HEK293T $ZAP^{-/-}$ and $TRIM25^{-/-}$. (B and C) To test if the RNA-binding domain of ZAP was sufficient to inhibit the replication of HIV-1_{CG}, we cotransfected HEK293T $ZAP^{-/-}$ cells with proviral plasmids encoding HIV-1_{WT} or HIV-1_{CG} and increasing amounts of plasmids (0, 72, 145 and 290 ng) encoding the full-length ZAP-L, a truncated form of ZAP lacking the RNA-binding domain (ΔZnF ZAP-L) and a truncated form of ZAP composed solely of the 254 N-terminal amino acids of ZAP (ZAP-N). After 48h, virus yield was measured and whole cell lysates were generated and analysed by SDS-PAGE and western blot.
(TIF)

S6 Fig. Co-expression of ZAP and TRIM25. (A and B) To assess if terminal modifications of TRIM25 would impact its antiviral activity, we cotransfected HEK293T $ZAP^{-/-}$ and $TRIM25^{-/-}$ cells with proviral plasmids encoding either HIV-1_{WT} or HIV-1_{CG} along with increasing amounts (0, 10, 20 or 90 ng) of N-terminally tagged TRIM25 (FLAG-TRIM25) or C-terminally tagged TRIM25 (TRIM25-HA). Forty-eight hours after transfection, viruses were harvested and titred onto MT4-R5-GFP cells while whole cells lysates of producer cells were generated and analyzed by western blot. (C) To evaluate if over-expression of TRIM25 would affect the expression levels of ZAP, we have co-transfected plasmids encoding ZAP chimeras with increasing amounts of plasmids encoding their cognate TRIM25. Cells were lysed 48h post-transfection and protein complexes were resolved and analyzed by SDS-PAGE/western blot. (D) Cells were transfected with human ZAP or avian ZAP chimeras along with proviral plasmids, as indicated in the main text. After 48h, whole cell lysates were generated, resolved by SDS-PAGE and analyses by western blot.
(TIF)

S7 Fig. Specificity of human and chicken ZAP against luciferase reporters. (A) HEK293T $ZAP^{-/-}$ and $TRIM25^{-/-}$ were co-transfected with luciferase reporters containing, as 3'UTRs, VSV-G wildtype sequences or CpG-enriched VSV-G sequences and plasmids encoding human and chicken ZAP and TRIM25. After 56h, cells were lysed and luciferase activity was measured. RLU, Relative light units.
(TIF)

S8 Fig. Comparison of the RNA-binding domains of human, chicken and alligator ZAP. (A) Protein sequence alignment of human, chicken and alligator N-terminal region. Zinc fingers are highlighted in solid line boxes while putative helices (1) and (2) are highlighted in dashed line boxes. Cov, percentage of sequence coverage; Pid, percentage of protein identity. (TIF)

Author Contributions

Conceptualization: Daniel Gonçalves-Carneiro, Paul D. Bieniasz.

Data curation: Daniel Gonçalves-Carneiro, Heley Ong, Amanda Shilton.

Formal analysis: Daniel Gonçalves-Carneiro.

Funding acquisition: Paul D. Bieniasz.

Investigation: Daniel Gonçalves-Carneiro, Matthew A. Takata, Heley Ong, Amanda Shilton.

Methodology: Daniel Gonçalves-Carneiro, Matthew A. Takata, Heley Ong.

Project administration: Paul D. Bieniasz.

Resources: Matthew A. Takata.

Software: Daniel Gonçalves-Carneiro.

Supervision: Paul D. Bieniasz.

Writing – original draft: Daniel Gonçalves-Carneiro.

Writing – review & editing: Daniel Gonçalves-Carneiro, Paul D. Bieniasz.

References

1. Chow KT, Gale M, Loo Y-M. RIG-I and Other RNA Sensors in Antiviral Immunity. Annu Rev Immunol [Internet]. 2018 Apr 20; 36(1):667–94. Available from: https://doi.org/10.1146/annurev-immunol-042617-053309 PMID: 29677479
2. Schoggins JW. Interferon-Stimulated Genes: What Do They All Do? Annu Rev Virol [Internet]. 2019 Sep 29; 6(1):567–84. Available from: https://doi.org/10.1146/annurev-virology-092818-015756 PMID: 31283436
3. Meyerson NR, Sawyer SL. Two-stepping through time: mammals and viruses. Trends Microbiol [Internet]. 2011/04/30. 2011 Jun; 19(6):286–94. Available from: https://pubmed.ncbi.nlm.nih.gov/21531564 https://doi.org/10.1016/j.tim.2011.03.006 PMID: 21531564
4. Gao G, Guo X, Goff SP. Inhibition of Retroviral RNA Production by ZAP, a CCCH-Type Zinc Finger Protein. Science (80-) [Internet]. 2002 Sep 6; 297(5587):1703 LP– 1706. Available from: http://science.sciencemag.org/content/297/5587/1703.abstract https://doi.org/10.1126/science.1074276 PMID: 12215647
5. Guo X, Carroll J-WN, MacDonald MR, Goff SP, Gao G. The Zinc Finger Antiviral Protein Directly Binds to Specific Viral mRNAs through the CCCH Zinc Finger Motifs. J Virol [Internet]. 2004 Dec 1; 78(23):12781 LP– 12787. Available from: http://jvi.asm.org/content/78/23/12781.abstract https://doi.org/10.1128/JVI.78.23.12781-12787.2004 PMID: 15542630
6. Müller S, Möller P, Bick MJ, Wurr S, Becker S, Günther S, et al. Inhibition of Filovirus Replication by the Zinc Finger Antiviral Protein. J Virol [Internet]. 2007 Mar 1; 81(5):2391 LP– 2400. Available from: http://jvi.asm.org/content/81/5/2391.abstract https://doi.org/10.1128/JVI.01601-06 PMID: 17182693
7. Li MMH, Lau Z, Cheung P, Aguilar EG, Schneider WM, Bozzacco L, et al. TRIM25 Enhances the Antiviral Action of Zinc-Finger Antiviral Protein (ZAP). PLOS Pathog [Internet]. 2017 Jan 6; 13(1):e1006145. Available from: https://doi.org/10.1371/journal.ppat.1006145 PMID: 28060952
8. Zheng X, Wang X, Tu F, Wang Q, Fan Z, Gao G. TRIM25 Is Required for the Antiviral Activity of Zinc Finger Antiviral Protein. Diamond MS, editor. J Virol [Internet]. 2017 May 1; 91(9):e00088–17. Available from: http://jvi.asm.org/content/91/9/e00088-17.abstract https://doi.org/10.1128/JVI.00088-17 PMID: 28202764

9. Guo X, Ma J, Sun J, Gao G. The zinc-finger antiviral protein recruits the RNA processing exosome to degrade the target mRNA. Proc Natl Acad Sci [Internet]. 2007 Jan 2; 104(1):151 LP– 156. Available from: http://www.pnas.org/content/104/1/151.abstract https://doi.org/10.1073/pnas.0607063104 PMID: 17185417

10. Ficarelli M, Wilson H, Pedro Galão R, Mazzon M, Antzin-Anduetza I, Marsh M, et al. KHNYN is essential for the zinc finger antiviral protein (ZAP) to restrict HIV-1 containing clustered CpG dinucleotides. Elife [Internet]. 2019 Jul 9;8. Available from: https://elifesciences.org/articles/46767 https://doi.org/10.7554/eLife.46767 PMID: 31284899

11. Takata MA, Gonçalves-Carneiro D, Zang TM, Soll SJ, York A, Blanco-Melo D, et al. CG dinucleotide suppression enables antiviral defence targeting non-self RNA. Nature. 2017; 550(7674). https://doi.org/10.1038/nature24039 PMID: 28953888

12. Meagher JL, Takata M, Gonçalves-Carneiro D, Keane SC, Rebendenne A, Ong H, et al. Structure of the zinc-finger antiviral protein in complex with RNA reveals a mechanism for selective targeting of CG-rich viral sequences. Proc Natl Acad Sci [Internet]. 2019 Nov 26; 116(48):24303 LP– 24309. Available from: http://www.pnas.org/content/116/48/24303.abstract https://doi.org/10.1073/pnas.1913232116 PMID: 31719195

13. Luo X, Wang X, Gao Y, Zhu J, Liu S, Gao G, et al. Molecular Mechanism of RNA Recognition by Zinc-Finger Antiviral Protein. Cell Rep [Internet]. 2020 Jan 7; 30(1):46–52.e4. Available from: https://doi.org/10.1016/j.celrep.2019.11.116 PMID: 31914396

14. Cooper DN, Gerber-Huber S. DNA methylation and CpG suppression. Cell Differ [Internet]. 1985; 17 (3):199–205. Available from: http://www.sciencedirect.com/science/article/pii/0045603985904889 https://doi.org/10.1016/0045-6039(85)90488-9 PMID: 3902251

15. Law JA, Jacobsen SE. Establishing, maintaining and modifying DNA methylation patterns in plants and animals. Nat Rev Genet [Internet]. 2010 Mar; 11(3):204–20. Available from: https://pubmed.ncbi.nlm.nih.gov/20142834 https://doi.org/10.1038/nrg2719 PMID: 20142834

16. Welsby I, Hutin D, Gueydan C, Kruys V, Rongvaux A, Leo O. PARP12, an interferon-stimulated gene involved in the control of protein translation and inflammation. J Biol Chem [Internet]. 2014/08/01. 2014 Sep 19; 289(38):26642–57. Available from: https://pubmed.ncbi.nlm.nih.gov/25086041 https://doi.org/10.1074/jbc.M114.589515 PMID: 25086041

17. Atasheva S, Frolova EI, Frolov I. Interferon-Stimulated Poly(ADP-Ribose) Polymerases Are Potent Inhibitors of Cellular Translation and Virus Replication. J Virol [Internet]. 2014 Feb 15; 88(4):2116 LP–2130. Available from: http://jvi.asm.org/content/88/4/2116.abstract https://doi.org/10.1128/JVI.03443-13 PMID: 24335297

18. Atasheva S, Akhrymuk M, Frolova EI, Frolov I. New PARP gene with an anti-alphavirus function. J Virol [Internet]. 2012/05/23. 2012 Aug; 86(15):8147–60. Available from: https://pubmed.ncbi.nlm.nih.gov/22623789 https://doi.org/10.1128/JVI.00733-12 PMID: 22623789

19. Li L, Zhao H, Liu P, Li C, Quanquin N, Ji X, et al. PARP12 suppresses Zika virus infection through PARP-dependent degradation of NS1 and NS3 viral proteins. Sci Signal [Internet]. 2018 Jun 19; 11 (535):eaas9332. Available from: https://pubmed.ncbi.nlm.nih.gov/29921658 https://doi.org/10.1126/scisignal.aas9332 PMID: 29921658

20. Pan D, Zhang L. Tandemly Arrayed Genes in Vertebrate Genomes. Bennetzen J, editor. Comp Funct Genomics [Internet]. 2008; 2008:545269. Available from: https://doi.org/10.1155/2008/545269

21. Sanchez JG, Sparrer KMJ, Chiang C, Reis RA, Chiang JJ, Zurenski MA, et al. TRIM25 Binds RNA to Modulate Cellular Anti-viral Defense. J Mol Biol [Internet]. 2018; 430(24):5280–93. Available from: http://www.sciencedirect.com/science/article/pii/S0022283618308477 https://doi.org/10.1016/j.jmb.2018.10.003 PMID: 30342007

22. Choudhury NR, Heikel G, Trubitsyna M, Kubik P, Nowak JS, Webb S, et al. RNA-binding activity of TRIM25 is mediated by its PRY/SPRY domain and is required for ubiquitination. BMC Biol [Internet]. 2017; 15(1):105. Available from: https://doi.org/10.1186/s12915-017-0444-9 PMID: 29117863

23. Jetz W, Thomas GH, Joy JB, Hartmann K, Mooers AO. The global diversity of birds in space and time. Nature [Internet]. 2012; 491(7424):444–8. Available from: https://doi.org/10.1038/nature11631 PMID: 23123857

24. Nielsen R, Bustamante C, Clark AG, Glanowski S, Sackton TB, Hubisz MJ, et al. A Scan for Positively Selected Genes in the Genomes of Humans and Chimpanzees. PLOS Biol [Internet]. 2005 May 3; 3(6): e170. Available from: https://doi.org/10.1371/journal.pbio.0030170 PMID: 15869325

25. Grunewald ME, Chen Y, Kuny C, Maejima T, Lease R, Ferraris D, et al. The coronavirus macrodomain is required to prevent PARP-mediated inhibition of virus replication and enhancement of IFN expression. PLOS Pathog [Internet]. 2019 May 16; 15(5):e1007756. Available from: https://doi.org/10.1371/journal.ppat.1007756 PMID: 31095648

26. Karlberg T, Klepsch M, Thorsell A-G, Andersson CD, Linusson A, Schüler H. Structural Basis for Lack of ADP-ribosyltransferase Activity in Poly(ADP-ribose) Polymerase-13/Zinc Finger Antiviral Protein. J Biol Chem [Internet]. 2015 Mar 20; 290(12):7336–44. Available from: http://www.jbc.org/content/290/12/7336.abstract https://doi.org/10.1074/jbc.M114.630160 PMID: 25635049

27. Kleine H, Poreba E, Lesniewicz K, Hassa PO, Hottiger MO, Litchfield DW, et al. Substrate-Assisted Catalysis by PARP10 Limits Its Activity to Mono-ADP-Ribosylation. Mol Cell [Internet]. 2008; 32(1):57–69. Available from: http://www.sciencedirect.com/science/article/pii/S1097276508005455 https://doi.org/10.1016/j.molcel.2008.08.009 PMID: 18851833

28. Bird AP, Taggart MH. Variable patterns of total DNA and rDNA methylation in animals. Nucleic Acids Res [Internet]. 1980 Apr 11; 8(7):1485–97. Available from: https://doi.org/10.1093/nar/8.7.1485 PMID: 6253937

29. Simmonds P, Xia W, Baillie JK, Mckinnon K. Modelling mutational and selection pressures on dinucleotides in eukaryotic phyla–selection against CpG and UpA in cytoplasmically expressed RNA and in RNA viruses. 2013;1–16.

30. Greenbaum BD, Levine AJ, Bhanot G, Rabadan R. Patterns of Evolution and Host Gene Mimicry in Influenza and Other RNA Viruses. PLOS Pathog [Internet]. 2008 Jun 6; 4(6):e1000079. Available from: https://doi.org/10.1371/journal.ppat.1000079 PMID: 18535658

31. Gu H, Fan RLY, Wang D, Poon LLM. Dinucleotide evolutionary dynamics in influenza A virus. Virus Evol [Internet]. 2019 Jul 1; 5(2). Available from: https://doi.org/10.1093/ve/vez038 PMID: 31737288

32. Babayan SA, Orton RJ, Streicker DG. Predicting reservoir hosts and arthropod vectors from evolutionary signatures in RNA virus genomes. Science (80-) [Internet]. 2018 Nov 2; 362(6414):577 LP– 580. Available from: http://science.sciencemag.org/content/362/6414/577.abstract https://doi.org/10.1126/science.aap9072 PMID: 30385576

33. Liberatore RA, Bieniasz PD. Tetherin is a key effector of the antiretroviral activity of type I interferon in vitro and in vivo. Proc Natl Acad Sci [Internet]. 2011 Oct 19;201113694. Available from: http://www.pnas.org/content/early/2011/10/18/1113694108.abstract https://doi.org/10.1073/pnas.1113694108 PMID: 22025715

34. Busnadiego I, Kane M, Rihn SJ, Preugschas HF, Hughes J, Blanco-Melo D, et al. Host and viral determinants of Mx2 antiretroviral activity. J Virol [Internet]. 2014/04/23. 2014 Jul; 88(14):7738–52. Available from: https://pubmed.ncbi.nlm.nih.gov/24760893 https://doi.org/10.1128/JVI.00214-14 PMID: 24760893

35. Suchard MA, Lemey P, Baele G, Ayres DL, Drummond AJ, Rambaut A. Bayesian phylogenetic and phylodynamic data integration using BEAST 1.10. Virus Evol [Internet]. 2018 Jun 8;4(1). Available from: https://doi.org/10.1093/ve/vey016 PMID: 29942656

36. Inoue JG, Miya M, Lam K, Tay B-H, Danks JA, Bell J, et al. Evolutionary Origin and Phylogeny of the Modern Holocephalans (Chondrichthyes: Chimaeriformes): A Mitogenomic Perspective. Mol Biol Evol [Internet]. 2010 Nov 1; 27(11):2576–86. Available from: https://doi.org/10.1093/molbev/msq147 PMID: 20551041

37. Simmonds P. SSE: a nucleotide and amino acid sequence analysis platform. BMC Res Notes [Internet]. 2012; 5(1):50. Available from: https://doi.org/10.1186/1756-0500-5-50 PMID: 22264264

38. Kutluay SB, Zang T, Blanco-Melo D, Powell C, Jannain D, Errando M, et al. Global Changes in the RNA Binding Specificity of HIV-1 Gag Regulate Virion Genesis. Cell [Internet]. 2014; 159(5):1096–109. Available from: http://www.sciencedirect.com/science/article/pii/S0092867414013014 https://doi.org/10.1016/j.cell.2014.09.057 PMID: 25416948